Computational Economics
https://doi.org/10.1007/s10614-025-11064-2

On the Estimation of Optimal Cutoffs for Power Laws and the Cross Section of Realized Foreign Exchange Rate Variances

Klaus Grobys[1,2]

Accepted: 14 July 2025

Abstract
Extending recent research, this study introduces a novel testing procedure based on modern block bootstrap techniques and maximum likelihood estimation to investigate whether the universal power-law process governing the cross-section of realized foreign exchange (FX) rate variances exhibits a conjoint cutoff. The analysis posits that the maximum likelihood estimator for the exponent of a power law is intrinsically dependent on the selected cutoff. Our innovative test, calibrated to the cross-section of realized daily FX variances, provides evidence for the existence of such a universal cutoff. The findings have significant implications for FX risk management. Specifically, they indicate that (a) the benefits of FX risk diversification may be more constrained than previously assumed, and (b) the extent of power-law behavior in the realized variance risk of the FX market may be substantially underestimated when conventional single-equation models are employed to determine the optimal cutoff for a power law.

Keywords Cutoff · Commonality · Foreign exchange rates · Power laws · Second moment · Variance

JEL Classification F31 · C22 · G11 · G12 · G13 · G15

✉ Klaus Grobys
klaus.grobys@uwasa.fi

[1] Finance Research Group, School of Accounting and Finance, University of Vaasa, Wolffintie 34, 65200 Vaasa, Finland

[2] Innovation and Entrepreneurship (InnoLab), University of Vaasa, Wolffintie 34, 65200 Vaasa, Finland

Published online: 05 September 2025

1 Introduction

Despite earlier well-established literature documenting that realized volatility approximates a lognormal distribution (e.g., Andersen et al., 2001a, b, c), accumulating evidence suggests that realized variances are better characterized by power laws. Grobys (2021) was among the first to fit power-law functions to the annualized daily realized variances of diverse asset classes, including gold and oil futures, Bitcoin, the S&P 500, and GBP/USD foreign exchange rates. The findings revealed that the power-law model could not be rejected for any of these asset markets. Intriguingly, the estimated power-law exponents varied significantly, providing statistical evidence that the variance of realized asset variances may be infinite.

Building on this foundation, Grobys (2023) analyzed data from May 16, 2006, to November 19, 2021, fitting power-law functions to the annualized daily realized variances of G10 currencies. The study found that estimated power-law exponents also indicated infinite variances for FX rates. While goodness-of-fit tests failed to reject the power-law model for at least seven out of nine realized FX variances, applying Bayes' rule demonstrated that the power-law model offered superior explanations for extreme events in realized FX variances. Further advancements were made by Fathi et al. (2024), who rigorously tested the power-law model against its lognormal counterpart using multiple goodness-of-fit tests applied to weekly realized FX variances for G10 currencies (sample: May 6, 2006, to December 29, 2023). The results corroborated previous findings, affirming that the power-law model more accurately describes the data-generating process. Consistent with Grobys (2023), Fathi et al. (2024) observed low power-law exponents, raising the question of whether realized FX variances are governed by a universal power-law behavior. Grobys (2024) addressed this question using realized daily FX variances for G10 currencies (May 16, 2006, to May 31, 2023) and proposed a test for invariance. The study aimed to determine whether a universal exponent governs the cross-section of realized FX variances over time and across various frequencies. The findings suggested the existence of such a universal exponent, with an estimated value notably low. However, a universal power-law process would also necessitate a shared cutoff defining the support of the power-law function. Determining this optimal cutoff remains challenging.

The importance of cutoff selection was underscored by Lux (2000), who attempted to replicate Krämer and Runde's (1996) estimation of the tail index for the German DAX and constituent stocks over the 1960–1992 sample. Lux attributed discrepancies in replication outcomes to differences in cutoff choices, highlighting the critical role of cutoff determination in power-law modeling. This growing body of literature reflects a paradigm shift toward understanding realized variances through the lens of power laws, underscoring their utility in modeling extreme events and advancing financial risk management.

Other recent literature investigates the behavior of jumps and volatility in financial markets using high-frequency data, with a focus on enhancing the accuracy of jump detection and volatility modeling. They emphasize the importance of advanced statistical or computational methods, such as marked Hawkes processes (Chen et al., 2024), machine learning algorithms (Uzun et al., 2023), and periodicity filters

(Yi, 2020, 2023, 2025), to refine the understanding of market dynamics. Uzun et al. (2023) and Yi (2020, 2023, 2025) focus on foreign exchange markets, employing methods like Lee and Mykland's jump detection to analyze intraday or daily jump probabilities. A consistent theme of this strand of literature is the use of volatility periodicity filters, which significantly reduce the probabilities of detected jumps, indicating the necessity of these filters for accurate modeling (Yi, 2020, 2023, 2024). Practical implications documented in this stream of literature are better hedging strategies (Uzun et al., 2023; Yi, 2023) or enhanced central bank policy frameworks (Uzun et al., 2023).

Overall, numerous research streams aim to model the variance of the FX market. Among these, the present study aligns most closely with the stream of research utilizing power laws (e.g., Fathi et al., 2024; Grobys, 2021, 2023, 2024). Recent literature has demonstrated that the cross-section of realized FX variances is governed by power laws exhibiting a statistically universal exponent (Grobys, 2024). The purpose of this study is to investigate whether this universal power-law process also features a common cross-sectional cutoff. Clarifying this issue is crucial because a common cross-sectional cutoff is essential to defining a universal power law comprehensively. To address this question, this study utilizes intraday price data for nine major currency pairs (AUD/USD, CAD/USD, CHF/USD, EUR/USD, GBP/USD, JPY/USD, NOK/USD, NZD/USD, and SEK/USD) spanning the period from January 16, 2015, to May 4, 2024. Intraday price quotations enable the computation of the Parkinson variance estimator for all FX data. Subsequently, modern blocks bootstrap methods are employed to estimate artificial datasets of realized daily FX variances. For each bootstrap replication, maximum likelihood estimation is used to derive the optimal power-law exponent and cutoff for all realized FX variance data vectors. This approach facilitates the computation of covariance matrices for both power-law exponents and cutoffs. Building on these estimations, the study revisits earlier research by testing whether the cross-section of realized FX variances is governed by a common power-law exponent. Furthermore, employing a similar hypothesis testing framework, the study examines whether a common cutoff exists. The present study argues that the presence of a universal cutoff, in conjunction with a universal power-law exponent, would hold significant implications for FX market risk management.

This study makes significant contributions to the existing literature on power laws and financial economics. First and foremost, although Taleb (2020) emphasizes that maximum likelihood estimation (MLE) is a robust methodology even in the presence of heavy tails—unlike ordinary least squares (OLS) or generalized method of moments (GMM) estimation—applying MLE to power-law functions introduces challenges due to the dependency of the power-law exponent on the cutoff. The Hill-plot (Clauset et al., 2009) visualizes this dependency by summarizing estimates of the exponent across a range of cutoffs. Given the variety of approaches proposed for optimal cutoff selection (e.g., Clauset et al., 2009), it is unsurprising that differences in cutoff choices lead to variations in estimated power-law exponents (Lux, 2000). Addressing these issues is crucial because accurate estimation of power-law parameters directly impacts the reliability of modeling extreme events in financial markets. By developing a statistical test derived from modern blocks bootstrap meth-

ods, this study provides a methodological advancement that enables more precise and consistent estimation across datasets. This contribution is particularly important for researchers and practitioners aiming to understand and manage risks in markets characterized by heavy-tailed distributions.

Furthermore, this study responds to the replication crisis highlighted by Hou et al. (2020), who argue that a significant portion of asset pricing studies fail to replicate. The importance of replication in scientific research cannot be overstated, as it ensures the validity and robustness of findings. Earlier research by Grobys (2023, 2024) and Fathi et al. (2024) used FX data beginning in 2006, a period during which not all G10 currencies were free-floating. This study's use of an updated dataset from January 16, 2015, to May 4, 2024, addresses this limitation by ensuring that all included currencies are in a state of free float. This refinement not only enhances the credibility of the findings but also sets a higher standard for future research in the field.

From a broader perspective, this research advances the literature on power laws in financial economics. Lux and Alfarano (2016) provide a comprehensive review of this area, which primarily relies on single-equation models, such as log–log regressions, to estimate power-law exponents. Breaking new ground, the present study adopts a multiple-equation approach, which significantly improves the robustness of statistical testing for commonalities in power-law behavior across multiple datasets. This methodological innovation has far-reaching implications for understanding systemic risks and market behaviors, as it allows for a more holistic analysis of interdependencies among financial assets. By expanding on Grobys (2024), who focused on universal power-law exponents, this research complements existing work by examining the equally critical aspect of common cutoffs. Such insights are invaluable for identifying universal patterns in financial data, which can inform better regulatory policies and risk management practices.

Finally, this study contributes to the literature on FX market risk. Previous works, such as Campbell et al. (2010), Opie and Riddiough (2020), and Della Corte et al. (2009), predominantly explored FX portfolios using correlation-based approaches. While correlation measures provide useful information, they often fail to capture the extreme tail risks that characterize FX markets. By following Mandelbrot's (1967) perspective and employing power-law principles, this study offers a novel lens through which to analyze FX market risks. This approach is critical for developing strategies that account for rare but impactful events, ultimately leading to more robust portfolio optimization and risk management. These contributions underscore the importance of this study in bridging theoretical advancements with practical applications, benefiting academics, practitioners, and policymakers alike.

Using data covering January 16, 2015, to May 4, 2024, the present study confirms earlier research by providing robust evidence for power-law behavior in realized daily FX variances (e.g., Fathi et al., 2024; Grobys, 2023, 2024). Specifically, for seven out of nine realized daily FX variances, the power-law null model cannot be rejected, as indicated by p-values ranging from 0.08 to 0.82. Estimates for power-law exponents derived from block bootstrapping suggests that, in practice, the variance of realized FX variances is infinite, consistent with earlier findings by Grobys (2023,

2024). The correlation matrix for power-law exponents, with an average correlation of 0.33, indicates a moderate level of dependency across datasets. Supporting Grobys (2024), the results show that all estimated correlations between power-law exponents are statistically significant and positive. These findings emphasize the necessity of accounting for the correlation matrix when conducting cross-sectional tests. Hypothesis testing further confirms the presence of a universal exponent governing the cross-section of realized FX variances. The correlation matrix for power-law cutoffs suggests a relatively low average correlation of 0.11. However, 27 out of 36 cutoff pairs exhibit positive and statistically significant correlations at the 5% level. This necessitates accounting for the correlation matrix of cutoffs in a manner analogous to the treatment of power-law exponents during hypothesis testing. Strikingly, the results suggest the existence of a universal cutoff, indicating that not only is the power-law exponent consistent across realized FX variances, but the function also exhibits a shared cutoff. Several robustness checks corroborate these findings. The implications for FX risk management are profound, as the results suggest that the benefits of risk diversification may be more limited than previously believed. Additionally, the scope of power-law behavior in the variance risk of the FX market could be significantly underestimated when using single-equation models to determine the optimal cutoff for the power-law function. These insights offer a refined perspective on modeling extreme risks in FX markets and highlight the importance of advanced statistical approaches in understanding variance dynamics.

This study is organized as follows: The next section described the data. The third section presents the methodology. The fourth section reports the results and the fifth section discusses the findings. The last section concludes.

2 Data

Publicly available intraday prices for the AUD/USD, CAD/USD, CHF/USD, EUR/USD, GBP/USD, JPY/USD, NOK/USD, NZD/USD, and SEK/USD exchange rates were downloaded from investing.com. This database provides us with FX quotations for daily open, high, and low prices. Unlike earlier research (e.g., Grobys, 2023; 2024; Fathi et al., 2024), this study employs data from January 16, 2015 to May 4, 2024 for the main analysis. Furthermore, only the intersection was employed—that is, only daily data are accounted for where all FX rates were quoted on the same day, leaving us with 2383 daily observations.

To estimate annualized daily variances, we employ the range-based variance estimator, proposed by Parkinson (1980), which is given by:

$$\sigma_{i,t}^2 = T\frac{1}{4\ln(2)}\left(\ln\left(\frac{H_{i,t}}{L_{i,t}}\right)\right)^2 = T\frac{1}{4\ln(2)}\left(\ln\left(H_{i,t}\right) - \ln\left(L_{i,t}\right)\right)^2, \tag{1}$$

where $H_{i,t}$ and $L_{i,t}$ denote the highest and lowest price for the FX rate i on trading day t, and $\sigma_{i,t}^2$ denotes the FX rate i's corresponding annualized daily variance, where

$T = 250$, as 250 trading days per annum are assumed.[1] The rationale for selecting a sample from January 16, 2015 to May 4, 2024.

is that we require that all G10 currencies should be in a state of free float which was ensured in the ex-post January 15, 2015 period. Specifically, on January 15, 2015, the Governing Board of the Swiss National Bank (SNB) decided to discontinue the minimum exchange rate of CHF 1.20 per euro. This exchange-rate peg was established in 2011 and abandoned without previous notice. Self-evidently, the pegging mechanism had also effects on the CHF/USD price fluctuations. To illustrate this issue, we plot in Fig. 1 in the appendix, the evolution of $\sigma^2_{CHF/USD,t}$ over the January, 2, 2001 to December, 17, 2002 period, whereas Fig. 2 in the appendix plots the evolution of $\sigma^2_{CHF/USD,t}$ over the January, 16, 2015 to March, 4, 2024 period. Visual inspection of Fig. 1 shows that this sample period cannot be deemed representative, as it deviates from the data evolution illustrated in Fig. 2 by a substantial margin. Specifically, the whole variation of the evolution of $\sigma^2_{CHF/USD,t}$ over the January, 2, 2001 to December, 17, 2002 period arises, in essence, from one outlier April 29, 2002 which corresponded to a 19.4-sigma event.[2] Interestingly, similar lacks of data representativeness could be observed for the $\sigma^2_{NOK/USD,t}$ or $\sigma^2_{SEK/USD,t}$ (unreported). As a consequence, the present study restricts the sample to a period where realized FX variances are "well-behaving," respectively, do not exhibit significant structural breaks in the data-generating processes.

Tables 1 reports the descriptive statistics for annualized daily realized FX variances. As shown in Table 1, the kurtosis values for the daily variance data vary between 42.7056 for the annualized daily CAD/USD variance and 1102.8090 for the annualized daily GBP/USD variance, suggesting extremely heavy tails. We also report the maxima in terms of sigma-events: We observe that the maximum realizations of annualized daily realized FX variances vary between 14- and incredible 39-sigma events—events that should be impossible to observe if the distributions governing realized FX variances followed the time-honored log-normal (e.g., Andersen et al., 2001a, b, c).

[1] For instance, recent studies from Grobys (2021; 2023; 2024) employ this variance estimator. The rationale for this choice is first, Chou et al.'s (2010) conclusion that range-based variance estimators comprise more information than changes in closing prices, and second, Shu and Zhang's (2006) finding that all types of range-based variance estimators perform very well. Furthermore, Grobys (2023; 2024) documents that the Parkinson variance estimator is less inflated than the Garman-Klass estimator which is manifested in lower maximum variance realizations produced from the Parkinson estimator.

[2] The corresponding Parkinson variance estimator has a value of $\sigma^2_{CHF/USD,April29,2002}$=1.52E-04 on that day. For the calculation of the 19.4-sigma event, data for $\sigma^2_{CHF/USD,t}$ over the January, 2, 2001 to December, 17, 2002 period was standardized. Furthermore, note that in Table 9 in the appendix we report the descriptive statistics for $\sigma^2_{CHF/USD,t}$ for various sample periods, that is, a first subsample period which is from January, 2, 2001 to December, 17, 2002, a second subsample which is from January, 2, 2001 to January, 14, 2015, and a third subsample (used as the main sample here) which is from January, 16, 2015 to March, 4, 2024. Unsurprisingly, the lack of variations in the ex-ante January 2015 period can be easily seen from the descriptive statistics, too.

Table 1 Descriptive statistics of daily range-based variances using the Parkinson-estimator

Publicly available intraday prices for the AUD/USD, CAD/USD, CHF/USD, EUR/USD, GBP/USD, JPY/USD, NOK/USD, NZD/USD, and SEK/USD exchange rates were downloaded from finance.yahoo.com. The sample period is from January, 16, 2015 to May, 4, 2024. Only the intersection of the data is employed; that is, only daily data are accounted for where all FX rates were quoted on the same day, leaving us with 2383 daily observations. To estimate annualized daily FX variances, the range-based variance estimator proposed by Parkinson (1980) is employed which is given by: $\sigma_{i,t}^2 = T\frac{1}{4\ln(2)}(\ln(H_{i,t}) - \ln(L_{i,t}))^2$,

where $H_{i,t}$ and $L_{i,t}$ denote the highest and lowest price for foreign exchange rate market i on trading day t, and $\sigma_{i,t}^2$ denotes foreign exchange rate market i's corresponding annualized realized variance where $T = 250$, as 250 trading days per annum are assumed. This table reports the descriptive statistics

	AUD/USD	CAD/USD	CHF/USD	EUR/USD	GBP/USD	JPY/USD	NOK/USD	NZD/USD	SEK/USD
Mean	0.0123	0.0060	0.0071	0.0068	0.0098	0.0079	0.0189	0.0131	0.0123
Median	0.0079	0.0040	0.0044	0.0042	0.0055	0.0041	0.0117	0.0086	0.0083
Maximum	0.5731	0.1042	0.1851	0.1977	1.4589	0.5085	0.9426	0.5564	0.5904
(in terms of σ)	(27.8965)	(14.2317)	(17.5947)	(18.7611)	(39.1265)	(28.8729)	(24.0802)	(26.7448)	(32.5860)
Minimum	0.0002	0.0000	0.0000	0.0000	0.0001	0.0000	0.0001	0.0003	0.0000
Std. Dev	0.0201	0.0069	0.0101	0.0102	0.0370	0.0173	0.0384	0.0203	0.0177
Skewness	13.5547	4.7998	7.4236	8.1790	30.6541	14.1607	15.1899	13.6739	16.6679
Kurtosis	303.4979	42.7056	91.9874	110.5473	1102.8090	329.8489	311.2849	304.1108	493.1843
Jarque–Bera (JB)	9038912.00	165686.70	808154.30	1175018.00	120000000.00	10686990.00	9528279.00	9076806.00	23968206.00
(p-value JB)	0.0000	0.0000	0.0000	0.0000	0.0000	0.0000	0.0000	0.0000	0.0000
Observations	2383	2383	2383	2383	2383	2383	2383	2383	2383

3 Econometric Methodology

3.1 Main Analysis

3.1.1 Power Laws

Following earlier research (Grobys, 2023, 2024; Fathi et al., 2024), we model annualized daily FX variances using the following power-law function:

$$p\left(x\right) = Cx^{-\alpha}, \tag{2}$$

where $C = \left(\alpha - 1\right) x_{MIN}^{\alpha-1}$ with $\alpha \in \{\mathbb{R}_+ \left| \alpha > 1 \right.\}$, $x = \sigma_{i,t}^2$ denotes the respective annualized daily FX variance i, provided that $x \in \{\mathbb{R}_+ \left| x_{MIN} \leq x < \infty \right.\}$, x_{MIN} is the minimum realization governed by the power-law, whereas α is the magnitude of the corresponding power-law exponent, which captures via extrapolation the low-probability deviation not seen in the data (Taleb, 2020).[3] It is important to note that this econometric model suggests the following functional form of the data-generating processes:

$$\sigma_{i,t}^2 = \left\{ \begin{array}{c} \sigma_{s_1,i,t}^2 \\ \sigma_{s_2,i,t}^2 \end{array} \right. , \text{ with } \boldsymbol{P} = \left(\begin{array}{cc} s_{1,i,t} \left| s_{1,i,t-1} \right. & s_{1,i,t} \left| s_{2,i,t-1} \right. \\ s_{2,i,t} \left| s_{1,i,t-1} \right. & s_{2,i,t} \left| s_{2,i,t-1} \right. \end{array} \right), \tag{3}$$

where $s_{1,i,t}$ denotes a state where FX variance i is governed by some thin-tailed process (e.g., log-normal), that is, $\sigma_{1,i,t}^2 \sim LGN(\mu_{1,i}, \sigma_{1,i}^2)$, whereas $s_{2,i,t}$ denotes a power law regime, that is, $\sigma_{2,i,t}^2 \sim PL(\alpha_{2,i}, x_{2,i,MIN})$, and $\boldsymbol{P}$ is the transition probability matrix. Note that Cirillo and Taleb (2020, p. 606) stress that "the more fat-tailed a statistical distribution, the more the 'tail wags the dog'. That is to say, more statistical information resides in the extremes and less in the 'bulk'—the events of high frequency—where it becomes almost noise." Therefore, in what follows, we exclusively focus our analysis on the tail of the distribution, that is, the region where the statistical signal resides and which is governed by a power-law process. What do we know about the relevant conditional moments? Given the functional form of Eq. (2), it can be shown that conditional moments of order k, $E\left[x \left| x > x_{MIN} \right.\right]$, are defined as:

$$E\left[X^k \left| x > x_{MIN} \right.\right] = \frac{\left(\alpha - 1\right)}{\left(\alpha - 1 - k\right)} x_{MIN}^k. \tag{4}$$

From Eq. (4) we see that the theoretical mean only exists for $\alpha > 2$, whereas the variance of realized FX variance only exists for $\alpha > 3$. Furthermore, from Eq. (4) it becomes evident that if $1 < \alpha \leq 2$, $E\left[x \left| x > x_{MIN} \right.\right] =]$[, and hence, $E\left[x\right] =]$[, which indicates the most extreme situation where the 'tail wags the dog.'

[3] Following Clauset et al. (2009), to simplify notation, index *i,* which denotes the respective individual FX variance, is dropped.

3.1.2 Maximum Likelihood Estimation and Goodness-of-Fit Test

Since maximum likelihood estimation (MLE) is the most accurate approach for estimating power-law exponents (Clauset et al., 2009; White et al., 2008), power-law exponents are estimated as:

$$\widehat{\alpha} = 1 + N\left(\sum\nolimits_{i=1}^{N} \ln\left(\frac{x_i}{x_{MIN}}\right)\right)^{-1}, \tag{5}$$

where $\widehat{\alpha}$ denotes the MLE estimator, N is the number of observations exceeding x_{MIN}, and other notations are as previously defined. Furthermore, Clauset et al. (2009) derive the corresponding standard deviation of the estimated power-law exponent:

$$\widehat{\sigma} = \frac{\widehat{\alpha} - 1}{\sqrt{N}} + O(\frac{1}{N}). \tag{6}$$

Because the MLE estimator depends on the chosen x_{MIN}, an essential question that arises is which candidate should be chosen for x_{MIN}? To optimize x_{MIN}, Clauset et al. (2009) propose an approach based on the optimal Kolmogorov–Smirnov (KS) distance *D*, which measures the maximum distance between the cumulative density functions (CDFs) of the data and the fitted power-law model as defined by:

$$D = MAX_{x \geq x_{MIN}} \left| S\left(x\right) - P(x) \right|, \tag{7}$$

where $S\left(x\right)$ is the CDF of the data for the observation with a value of at least x_{MIN}, and $P(x)$ is the CDF for the power-law model that best fits the data in the region $x \geq x_{MIN}$. The optimal $\widehat{x}_{MIN}$ is then the value of x_{MIN} that minimizes *D*. Clauset et al. (2009) provide strong evidence that their proposed approach to select the optimal x_{MIN} outperforms traditional log–log regressions by a substantial margin; however, as pointed out in Grobys (2024), their proposed approach is only applicable to a single data series.

To analyze whether the power-law model given by the parameter vector $(\widehat{\alpha}, \widehat{x}_{MIN})$ is reasonable, this study uses the goodness-of-fit test (GoF), as derived from Clauset et al. (2009). This GoF produces a *p*-value that quantifies the plausibility of the power-law null model by comparing *D* from Eq. (7) with distance measurements for comparable synthetic data sets drawn from the hypothesized model, generated by the parameter vector $(\widehat{\alpha}, \widehat{x}_{MIN})$. The *p*-value is calculated as the fraction of synthetic distances that exceed the empirical distance. Making use of a common significance level of 5%, the power-law null model is not rejected, as the difference between the empirical data and the model can be attributed to statistical fluctuations.[4]

[4] The GoF test is detailed in Clauset et al. (2009).

3.1.3 Computing Expected First and Second Moments and Covariance Matrices via Blocks Bootstraps

Whereas methodologies proposed in the literature to estimate power-law exponents (e.g., Clauset et al., 2009) were designed for analyzing a single data series or a seemingly unrelated data series, a recent study of Grobys (2024) proposes a new approach incorporating blocks bootstraps to estimate the covariance matrix of power-law exponents for multiple seemingly unrelated data. He shows that power-law exponents for realized foreign exchange rate variances are indeed correlated which implies that the covariance matrix of power-law exponents needs to be accounted for when implementing joint tests. Utilizing this approach incorporating block bootstraps, we explore whether (a) the cutoffs for power-law functions are correlated, and (b) whether a common cutoff exists across power-law functions governing FX variances. If FX variances exhibited not only a common power-law exponent but also a common cutoff would suggest a universal power-law behavior of the variance risk in the FX market.

To explore this issue, a blocks bootstrap procedure, as proposed in Grobys (2024), is implemented. Denoting the selected block length as m, a blocks bootstrap procedure is chosen such that $E[m] = \sqrt{T}$. Then the Tx1 data vectors of FX variances $i = 1, \ldots, N$, denoted as $\boldsymbol{x}_i$, are stacked into matrix $\boldsymbol{Y}$:

$$\boldsymbol{Y} = [\boldsymbol{x}_1, \boldsymbol{x}_2, \ldots, \boldsymbol{x}_N].$$

The blocks of the dimension *m*xN are randomly drawn from matrix $\boldsymbol{Y}$ with respect to the time dimension $t = 1, \ldots, T$. These blocks are governed by a geometric distribution—that is, $m \sim GEO(p)$ with $E[m] = \frac{(1-p)}{p}$. Drawing geometrically-distributed random blocks ensures that the variance data are stationarity (Godfrey, 2009). Since our data has a length of 2383 implying $\sqrt{T} \approx 49$, we use $E[m] = 49$, $p = 0.0200$. Note that the blocks drawn from $\boldsymbol{Y}$ vary in lengths. The randomly drawn blocks, m, which have dimensions *m*xN from data matrix $\boldsymbol{Y}$, are stacked in matrix $\boldsymbol{Y}_b$ as:

$$\boldsymbol{Y}_b = \begin{bmatrix} m_1 \\ m_2 \\ m_3 \\ \vdots \end{bmatrix}.$$

The procedure is stopped when the length of the artificial matrix $\boldsymbol{Y}_b$ exhibits a length exceeding T. Observations exceeding T are cut off to ensure that the artificial data matrix $\boldsymbol{Y}_b$ has the same length as the original data matrix $\boldsymbol{Y}$. This process corresponds to one iteration b of the blocks bootstrap procedure. Employing this blocks bootstraps, for each iteration b, the Tx1 vectors,$\boldsymbol{x}_{b,1}$, $\boldsymbol{x}_{b,2}$, …, $\boldsymbol{x}_{b,N}$ are extracted from matrix $\boldsymbol{Y}_b$, and the MLE estimators are estimated using the procedure described in the previous section giving us:

$$\begin{bmatrix} \widehat{\alpha}_{b,1} & \widehat{\alpha}_{b,2} & \cdots & \widehat{\alpha}_{b,N} \end{bmatrix}, \text{ and}$$
$$\begin{bmatrix} \widehat{x}_{MIN,b,1} & \widehat{x}_{MIN,b,2} & \cdots & \widehat{x}_{MIN,b,N} \end{bmatrix}.$$

This blocks bootstrap procedure is performed using $b = 1, \ldots, 1000$ iterations and point estimates are stacked into BxN matrices $\widehat{\boldsymbol{\alpha}}_{BOOT}$ and $\widehat{\boldsymbol{x}}_{MIN,BOOT}$:

$$\widehat{\boldsymbol{\alpha}}_{BOOT} = \begin{pmatrix} \widehat{\alpha}_{1,1} & \widehat{\alpha}_{1,2} & \cdots & \cdots & \widehat{\alpha}_{1,N} \\ \widehat{\alpha}_{2,1} & \widehat{\alpha}_{1,2} & \cdots & \cdots & \widehat{\alpha}_{2,N} \\ \vdots & \vdots & \vdots & \vdots & \vdots \\ \vdots & \vdots & \vdots & \vdots & \vdots \\ \widehat{\alpha}_{B,1} & \widehat{\alpha}_{B,2} & \cdots & \cdots & \widehat{\alpha}_{B,N} \end{pmatrix}, \text{ and}$$

$$\widehat{\boldsymbol{x}}_{MIN,BOOT} = \begin{pmatrix} \widehat{x}_{MIN,1,1} & \widehat{x}_{MIN,1,2} & \cdots & \cdots & \widehat{x}_{MIN,1,N} \\ \widehat{x}_{MIN,2,1} & \widehat{x}_{MIN,1,2} & \cdots & \cdots & \widehat{x}_{MIN,2,N} \\ \vdots & \vdots & \vdots & \vdots & \vdots \\ \vdots & \vdots & \vdots & \vdots & \vdots \\ \widehat{x}_{MIN,B,1} & \widehat{x}_{MIN,B,2} & \cdots & \cdots & \widehat{x}_{MIN,B,N} \end{pmatrix}.$$

The corresponding bootstrapped standard errors $\widehat{\sigma}_{\widehat{\alpha}_{BOOT},i}$ and $\widehat{\sigma}_{\widehat{x}_{MIN,BOOT},i}$ are then given by:

$$\widehat{\sigma}_{\widehat{\alpha}_{BOOT},i} = \sqrt{\frac{1}{B}\sum_{b=1}^{B}\left(\widehat{\alpha}_{b,i} - \overline{\widehat{\alpha}}_{b,i}\right)^2}, \text{ and}$$
$$\widehat{\sigma}_{\widehat{x}_{MIN,BOOT},i} = \sqrt{\frac{1}{B}\sum_{b=1}^{B}\left(\widehat{x}_{MIN,b,i} - \overline{\widehat{x}}_{MIN,b,i}\right)^2}.$$

According to Grobys and Junttila (2021), this approach is robust to unknown dependency structures in the data, which are commonly observed for financial data.[5] Since this blocks bootstrap approach retains co-dependencies across the data, it enables us to compute the following covariances using the matrices $\widehat{\boldsymbol{\alpha}}_{BOOT}$ and $\widehat{\boldsymbol{x}}_{MIN,BOOT}$:

$$\widehat{\sigma}_{\widehat{\alpha}_{BOOT},i,j} = \frac{1}{B}\sum_{b=1}^{B}\left(\widehat{\alpha}_{b,i} - \overline{\widehat{\alpha}}_{b,i}\right)\left(\widehat{\alpha}_{b,j} - \overline{\widehat{\alpha}}_{b,j}\right) \text{ with } i \neq j,$$

$$\widehat{\sigma}_{\widehat{x}_{MIN,BOOT},i,j} = \frac{1}{B}\sum_{b=1}^{B}\left(\widehat{x}_{MIN,b,i} - \overline{\widehat{x}}_{MIN,b,i}\right)\left(\widehat{x}_{MIN,b,j} - \overline{\widehat{x}}_{MIN,b,j}\right) \text{ with } i \neq j,$$

[5] Furthermore, the methodology proposed in the study of Clauset et al. (2009) relies on the assumption of independency which is not satisfied due to conditional heteroskedasticity. Consequently, standard deviations for estimated power-law exponents, as given by Eq. (6), must be biased. Modern blocks bootstrap addresses this issue by providing standard deviations that are robust to unknown dependency structures in the data. Note that the findings documented in the recent study of Grobys' (2024) indicate that standard deviations for estimated power-law exponents derived from blocks bootstrap are substantially larger than those obtained from using Clauset et al.'s (2009) approach.

for $i, j = 1, \ldots, N$. The corresponding NxN covariance matrices are then $COV(\widehat{\boldsymbol{\alpha}}_{BOOT})$, and $COV(\widehat{\boldsymbol{x}}_{MIN,BOOT})$, respectively. As noted in Grobys (2024), if covariances are statistically significant, the covariance matrices need to be accounted for when implementing statistical tests for detecting potential commonalities across the FX variances.

3.1.4 Is there a Common Exponent Governing Power Law Functions of FX Variances?

To explore whether a common component governing power-law behavior of FX variances exists, We follow Grobys (2024) and employ the following test statistic:

$$\widehat{\lambda} = (\dot{\boldsymbol{\alpha}} - q1)\prime \widehat{\boldsymbol{\Sigma}}_{\widehat{\boldsymbol{\alpha}}}^{-1} (\dot{\boldsymbol{\alpha}} - q1), \tag{8}$$

where the covariance matrix $\widehat{\boldsymbol{\Sigma}}_{\widehat{\boldsymbol{\alpha}}} = COV(\widehat{\boldsymbol{\alpha}}_{BOOT})$, has the dimension NxN, $\dot{\boldsymbol{\alpha}}$ is a vector of dimension Nx1 stacking consistent estimates for power-law exponents in a column vector, 1 is a Nx1 vector consisting of ones, and q is the hypothesized common power-law exponent. The estimated test statistic, denoted as $\widehat{\lambda}$, is under the null hypothesis distributed as $\chi^2(N)$. Following Grobys (2024), the test statistic is iteratively estimated covering the economically important interval $q = (2.1, 2.2, \ldots, 3.1)$. Since power-law exponents for nine FX variances are tested, the corresponding test statistic is under the null hypothesis distributed as $\chi^2(9)$. Using a statistical significance level of 5% level, the null hypothesis is not rejected for $\widehat{\lambda} < 16.92$. Note that according to Eq. (8), rejection of the null hypothesis $\boldsymbol{\alpha}' = q1 \; \forall \; q = (2.1, 2.2, \ldots, 3.1)$ would indicate that the FX variances exhibit heterogenous sources of risk manifested in FX-specific power-law behavior.

3.1.5 Is there a Common Cutoff Associated with Power-Law Functions for FX Variances?

Earlier research focused on examining commonalities in power-law exponents (Grobys, 2024). Extending this research, here we explore whether the power-law functions governing realized FX variances exhibit a common cutoff. This is an important issue because Lux (2000) highlights that documented results of studies on power laws in financial economics depend on the chosen cutoff. Relatedly, Lux (2000, p. 646) points out that in "[i]n view of these problems of implementations, the recent development of methods for *data-driven* selection of the tail sample constitutes an important advance." Therefore, to address this issue, the present study employs a chi-square-type distribution in search of a common cutoff for multiple data vectors of FX variances. To do so, the following test statistic is proposed:

$$\widehat{\lambda} = (\dot{\boldsymbol{x}}_{MIN} - r1)\prime \widehat{\boldsymbol{\Sigma}}_{\widehat{\boldsymbol{x}}_{MIN}}^{-1} (\dot{\boldsymbol{x}}_{MIN} - r1), \tag{9}$$

where the covariance matrix $\widehat{\boldsymbol{\Sigma}}_{\widehat{\boldsymbol{x}}_{MIN}} = COV(\widehat{\boldsymbol{x}}_{MIN,BOOT})$, has the dimension NxN, $\dot{\boldsymbol{x}}_{MIN}$ is a vector of dimension Nx1 stacking consistent estimates for cutoffs

in a column vector, 1 is a Nx1 vector consisting of ones, and r is the hypothesized common cutoff. The estimated test statistic denoted as $\widehat{\lambda}$ is under the null hypothesis distributed as $\chi^2(N)$. The test statistic is iteratively estimated covering the full range of estimated cutoffs, that is, the hypothesis tests are implemented on the interval $r = (0.007,0.008,0.009,\ldots,0.034,0.035)$. Since cutoffs for power-law functions of nine realized FX variances are tested, the corresponding test statistic is under the null hypothesis distributed as $\chi^2(9)$. Again, using a statistical significance level of 5% level, the null hypothesis is not rejected for $\widehat{\lambda} < 16.92$. Rejecting the null hypothesis $(\dot{\boldsymbol{x}}_{MIN} - r1)\forall\ r = (0.007,0.008,0.009,\ldots,0.034,0.035)$ would indicate that the FX variances exhibit FX variance risk-specific cutoffs.

4 Results

4.1 Main Results

Table 2 reports the results from estimating the power-law exponents for daily variances based on the Parkinson-estimator using the MLE approach proposed by Clauset et al. (2009). The sample period is from January, 16, 2015 to May, 4, 2024, comprising 2383 daily observations. We observe from Table 2 that the estimated power-law exponents vary between $\widehat{\alpha} = 2.6400$ for the annualized daily JPY/USD variance and $\widehat{\alpha} = 3.5709$ for the annualized daily SEK/USD variance. The fraction of observations governed by power-law processes varies between 6.67 percent for the annualized daily SEK/USD variance and 26.81 percent for the annualized daily JPY/USD variance. These figures are close to the ones reported in Grobys (2023) who examines power-law behavior of annualized daily variances for G10 currencies using a sample May 16, 2006 to November 19, 2021. Specifically, Grobys (2023) finds that estimated power-law exponents range between $\widehat{\alpha} = 2.25$ and $\widehat{\alpha} = 2.78$ for annualized daily AUD/USD variance and annualized daily EUR/USD variance, respectively.

Furthermore, implementing the Clauset et al.'s (2009) GoF test, the evidence suggests that the power-law null model cannot be rejected for seven-out-of-nine annualized daily FX variances.[6] This result is also in line with Grobys (2023). On the other hand, our findings suggest that the power-law null model is rejected for annualized daily JPY/USD and CAD/USD variances, whereas Grobys' (2023) findings suggest that the power-law null model is rejected for annualized daily SEK/USD and CAD/USD variances. An explanation for the discrepancy between the findings could be the chosen sample which, in turn, confirms Taleb's (2012) argument that absence of evidence for power-law behavior doesn't imply evidence for absence of power-law behavior.

Whereas the point estimates for power-law exponents derived from MLE should be unbiased, the parameter uncertainty will be underestimated in the presence of dependency structures. Since volatility clustering is a stylized fact of financial data and therefore gives reasons for long-range dependence in the variance processes, we employ block bootstraps to estimate robust parameter variances. Following Grobys

[6] To implement the GoF tests, we used 500 iterations for each hypothesis test.

Table 2 Estimated power-law functions for daily FX variances

Daily FX variances are modeled using the following power-law function: $p\left(x\right)=Cx^{-\alpha}$, where $C=\left(\alpha-1\right)x_{MIN}^{\alpha-1}$ with $\alpha\in\{\mathbb{R}_{+}\,|\alpha\,>1\}$, x denotes the respective annualized daily or weekly FX variance provided $x\in\{\mathbb{R}_{+}\,|x_{MIN}\leq x<\infty\}$, x_{MIN} is the minimum value governed by the power-law process, and α is the magnitude of the corresponding tail exponent. The power-law exponents are estimated as: $\widehat{\alpha}=1+N\left(\sum_{i=1}^{N}\ln\left(\frac{x_i}{x_{MIN}}\right)\right)^{-1}$, where $\widehat{\alpha}$ denotes the MLE estimator, N is the number of observations exceeding x_{MIN}, and other notations are as previously defined. The estimate $\widehat{\alpha}$ is selected based on the optimal Kolmogorov–Smirnov (KS) distance D measuring the maximum distance between the cumulative density functions (CDFs) of the data and the fitted power-law model as defined by: $D=MAX_{x\geq x_{MIN}}\left|S\left(x\right)-P(x)\right|$, where $S\left(x\right)$ is the CDF of the data for the observation with a value of at least x_{MIN}, and $P(x)$ is the CDF for the power-law model that best fits the data in the region $x\geq x_{MIN}$. Estimate $\widehat{x}_{MIN}$ is then the value of x_{MIN} that minimizes D. This table reports the estimates $\widehat{\alpha}$, $\widehat{x}_{min}$, $\widehat{\sigma}$, and N for daily FX variance data. Also, the p-values for goodness-of-fit (GoF) tests are reported that test estimated power-law models under the null hypotheses. We used 500 iterations to implement the tests. The sample period is from January, 16, 2015 to May, 4, 2024, comprising 2383 daily observations

	$\widehat{\sigma}^2_{AUD/USD}$	$\widehat{\sigma}^2_{CAD/USD}$	$\widehat{\sigma}^2_{CHF/USD}$	$\widehat{\sigma}^2_{EUR/USD}$	$\widehat{\sigma}^2_{GBP/USD}$	$\widehat{\sigma}^2_{JPY/USD}$	$\widehat{\sigma}^2_{NOK/USD}$	$\widehat{\sigma}^2_{NZD/USD}$	$\widehat{\sigma}^2_{SEK/USD}$
$\widehat{\alpha}$	3.1018	3.0591	2.7798	2.8030	2.7187	2.6400	3.0229	3.0482	3.5709
$\widehat{x}_{min}$	0.0211	0.0085	0.0090	0.0093	0.0126	0.0078	0.0318	0.0197	0.0320
$\widehat{\sigma}$	0.1713	0.1393	0.1183	0.1310	0.1341	0.1044	0.1692	0.1534	0.2832
N (N in %)	328 (13.76%)	482 (20.23%)	552 (23.16%)	458 (19.22%)	411 (17.25%)	639 (26.81%)	319 (13.39%)	395 (16.58%)	159 (6.67%)
p-value (GoF)	0.5260	0.0300	0.1340	0.0820	0.8160	0.0060	0.3440	0.4260	0.5940

(2024), we employ an expected block length of $\sqrt{T}$ and because $T = 2383$, it follows that $\sqrt{T} \approx 49$, we hence $E[m] = 49$, and $p = 0.0200$. The blocks bootstraps procedure allows us to estimate the distributions for both power-law exponents and cutoffs. The results derived from 1000 bootstrap replications are reported in Tables 3 and 4. From Table 3 we observe that the average point estimates for bootstrapped power-law exponents are close to the ones reported in Table 2. This should not come as a surprise because both estimates should be unbiased. As an example, the estimated power-law exponent for annualized daily AUD/USD variance is $\widehat{\alpha} = 3.1018$ based on the MLE approach in line with Clauset et al. (2009), and $\widehat{\alpha} = 3.1019$ based on our blocks bootstraps approach. Whereas the point estimates are virtually the same, the parameter uncertainty is not: We see from Table 2 that Clauset et al.'s (2009) estimate—which is derived under the IID assumption—suggests that $\widehat{\sigma} = 0.1713$, whereas our robust estimate for parameter uncertainty suggests that $\widehat{\sigma}_{\widehat{\alpha}_{BOOT}} = 0.4232$. That is, our robust estimate suggests the parameter uncertainty to be ≈ 2.5 times higher than under the IID assumption.

Self-evidently, this is an important issue for hypothesis tests. For instance, according to Table 2, the estimated power-law exponent for annualized daily SEK/USD variance, estimated at $\widehat{\alpha} = 3.5709$ is $2.02\widehat{\sigma}$ above a hypothesized $\widehat{\alpha} = 3$. That means, a hypothesis test based on the IID assumption would mistakenly result in rejecting the null hypothesis that the variance of annualized daily SEK/USD variance exists, which is obviously the case if the null hypothesis $\widehat{\alpha} = 3$ or $\widehat{\alpha} \leq 3$ is rejected. On the other hand, our robust estimate suggests that $\widehat{\alpha} = 3.5709$ is only $1.42\widehat{\sigma}_{\widehat{\alpha}_{BOOT}}$ above a hypothesized $\widehat{\alpha} = 3$ implying that a hypothesized $\widehat{\alpha} = 3$ could not be rejected. Overall, disregarding from dependency structures in the data might lead to misleading results derived from methodologies relying on the IID assumption.

Extending Grobys' (2024) study, we use blocks bootstraps to estimate the distribution for cutoffs. From Table 4 that average values for cutoffs range between $\widehat{x}_{MIN} = 0.0085$ and $\widehat{x}_{MIN} = 0.0289$ for the power-law function for annualized daily JPY/USD variance and annualized daily NOK/USD variance, respectively.[7] Moreover, the bootstrap procedure suggests that the cutoff uncertainty varies between $\widehat{\sigma}_{\widehat{x}_{MIN,BOOT}} = 0.0024$ and $\widehat{\sigma}_{\widehat{x}_{MIN,BOOT}} = 0.0083$ for the power-law function for the annualized daily CAD/USD variance and annualized daily SEK/USD variance, respectively. It is important to note that the distribution for $\widehat{x}_{MIN}$ is not analytically deducible, yet modern blocks bootstraps allows us to estimate the relevant distributional metrics. The corresponding (robust) *t*-statistics vary between 2.53 and 4.95 for the average cutoffs for the annualized daily SEK/USD variance and annualized daily NZD/USD variance, respectively. This suggests that the average cutoffs retrieved from blocks bootstraps are statistically significant on at least a 5% level.

Is FX variance risk governed by a common factor? Grobys' (2024) study shows that annualized daily FX variances are indeed governed by such a universal exponent corresponding to $\alpha^* \approx 2.6$ which is line with the theory of complex systems. To revisit this issue, we compute the covariance matrix via blocks bootstraps using $E[m] = 49$, and $p = 0.0200$. The estimated correlation matrix for power-law expo-

[7] Note that we again make use of $E[m] = 49$, and $p = 0.0200$.

Table 3 Descriptive statistics of power-law exponent distributions derived from blocks bootstraps

We implement a blocks bootstrap procedure, as proposed in Grobys (2024). Denoting the selected block length as m, a blocks bootstrap procedure is chosen such that $E[m] = \sqrt{T}$. Then the Tx1 data vectors of FX variances $i = 1, \ldots, N$, denoted as $\boldsymbol{x}_i$, are stacked into matrix $\boldsymbol{Y}$: $\boldsymbol{Y} = [\boldsymbol{x}_1, \boldsymbol{x}_2, \ldots, \boldsymbol{x}_N]$.

The blocks of the dimension mxK are randomly drawn from matrix $\boldsymbol{Y}$ with respect to the time dimension $t = 1, \ldots, T$. These blocks are governed by a geometric distribution—that is, $m \sim GEO(p)$ with $E[m] = \frac{(1-p)}{p}$. Drawing geometrically-distributed random blocks ensures that the variance data are stationarity (Godfrey, 2009). Since our data has a length of 2383 implying $\sqrt{T} \approx 49$, we use $E[m] = 49, p = 0.0200$. Note that the blocks drawn from $\boldsymbol{Y}$ vary in lengths. The randomly drawn blocks, m, which have dimensions mxK from data matrix $\boldsymbol{Y}$, are stacked in matrix $\boldsymbol{Y}_b$ as: $\boldsymbol{Y}_b = \begin{bmatrix} m_1 \\ m_2 \\ m_3 \\ \vdots \end{bmatrix}$.

The procedure is stopped when the length of the artificial matrix $\boldsymbol{Y}_b$ exhibits a length exceeding T. Observations exceeding T are cut off to ensure that the artificial data matrix $\boldsymbol{Y}_b$ has the same length as the original data matrix $\boldsymbol{Y}$. This process corresponds to one iteration b of the blocks bootstrap procedure. Employing this blocks bootstraps, for each iteration b, the Tx1 vectors,$\boldsymbol{x}_{b,1}$, $\boldsymbol{x}_{b,2}$, …, $\boldsymbol{x}_{b,N}$ are extracted from matrix $\boldsymbol{Y}_b$, and the MLE estimators for power-law exponents are estimated using the procedure described in Section. 3, giving us: $\begin{bmatrix} \widehat{\alpha}_{b,1} & \widehat{\alpha}_{b,2} & \cdots & \widehat{\alpha}_{b,N} \end{bmatrix}$.

This blocks bootstrap procedure is performed using $b = 1, \ldots, 1000$ iterations and point estimates are stacked into BxN matrix $\widehat{\boldsymbol{\alpha}}_{BOOT}$:

$$\widehat{\boldsymbol{\alpha}}_{BOOT} = \begin{pmatrix} \widehat{\alpha}_{1,1} & \widehat{\alpha}_{1,2} & \cdots & \cdots & \widehat{\alpha}_{1,N} \\ \widehat{\alpha}_{2,1} & \widehat{\alpha}_{1,2} & \cdots & \cdots & \widehat{\alpha}_{2,N} \\ \vdots & \vdots & \vdots & \vdots & \vdots \\ \vdots & \vdots & \vdots & \vdots & \vdots \\ \widehat{\alpha}_{B,1} & \widehat{\alpha}_{B,2} & \cdots & \cdots & \widehat{\alpha}_{B,N} \end{pmatrix}.$$

The corresponding bootstrapped standard errors $\widehat{\sigma}_{\widehat{\alpha}_{BOOT},i}$ are then given by: $\widehat{\sigma}_{\widehat{\alpha}_{BOOT},i} = \sqrt{\frac{1}{B}\sum_{b=1}^{B}\left(\widehat{\alpha}_{b,i} - \overline{\widehat{\alpha}}_{b,i}\right)^2}$. This table reports the descriptive statistics for the power-law exponent distributions derived from blocks bootstraps

$\widehat{\alpha}$ stats for $\widehat{\sigma}_i^2$:	$\widehat{\sigma}^2_{AUD/USD}$	$\widehat{\sigma}^2_{CAD/USD}$	$\widehat{\sigma}^2_{CHF/USD}$	$\widehat{\sigma}^2_{EUR/USD}$	$\widehat{\sigma}^2_{GBP/USD}$	$\widehat{\sigma}^2_{JPY/USD}$	$\widehat{\sigma}^2_{NOK/USD}$	$\widehat{\sigma}^2_{NZD/USD}$	$\widehat{\sigma}^2_{SEK/USD}$
Mean	3.1019	3.2096	2.9143	2.9278	2.7316	2.4772	3.1003	3.0968	3.2338
Median	3.0564	3.1689	2.8886	2.9007	2.6982	2.4569	2.9886	3.0646	3.2668

Table 3 (continued)

$\widehat{\alpha}$ stats for $\widehat{\sigma}_i^2$:	$\widehat{\sigma}^2_{AUD/USD}$	$\widehat{\sigma}^2_{CAD/USD}$	$\widehat{\sigma}^2_{CHF/USD}$	$\widehat{\sigma}^2_{EUR/USD}$	$\widehat{\sigma}^2_{GBP/USD}$	$\widehat{\sigma}^2_{JPY/USD}$	$\widehat{\sigma}^2_{NOK/USD}$	$\widehat{\sigma}^2_{NZD/USD}$	$\widehat{\sigma}^2_{SEK/USD}$
Maximum	4.8859	4.6150	3.9391	4.0336	3.6603	3.1360	5.6617	4.6426	4.6656
Minimum	2.2610	2.6360	2.5271	2.5075	2.2465	2.1254	2.3378	2.5870	2.3635
Std. Dev	0.4232	0.3162	0.1830	0.1984	0.2184	0.1440	0.4860	0.2492	0.4009
Skewness	0.9767	0.9063	1.2854	1.0090	0.8459	1.0886	1.3789	1.1339	−0.0098
Kurtosis	4.5814	4.1998	6.4132	5.0203	4.1336	5.0630	5.2928	5.7265	2.7134
Jarque–Bera (JB)	263.20	196.87	760.79	339.74	172.82	374.85	535.96	524.04	3.44
p-value (JB)	0.0000	0.0000	0.0000	0.0000	0.0000	0.0000	0.0000	0.0000	0.1792
Observations	1000	1000	1000	1000	1000	1000	1000	1000	1000

Table 4 Descriptive statistics of cutoff distributions derived from blocks bootstraps

We implement a blocks bootstrap procedure, as proposed in Grobys (2024). Denoting the selected block length as m, a blocks bootstrap procedure is chosen such that $E[m] = \sqrt{T}$. Then the Tx1 data vectors of FX variances $i = 1, \ldots, N$, denoted as $\boldsymbol{x}_i$, are stacked into matrix $\boldsymbol{Y}$: $\boldsymbol{Y} = [\boldsymbol{x}_1, \boldsymbol{x}_2, \ldots, \boldsymbol{x}_N]$.

The blocks of the dimension *m*xK are randomly drawn from matrix $\boldsymbol{Y}$ with respect to the time dimension $t = 1, \ldots, T$. These blocks are governed by a geometric distribution—that is, $m \sim GEO(p)$ with $E[m] = \frac{(1-p)}{p}$. Drawing geometrically-distributed random blocks ensures that the variance data are stationarity (Godfrey, 2009). Since our data has a length of 2383 implying $\sqrt{T} \approx 49$, we use $E[m] = 49, p = 0.0200$. Note that the blocks drawn from $\boldsymbol{Y}$ vary in lengths. The randomly drawn blocks, m, which have dimensions *m*xK from data matrix $\boldsymbol{Y}$, are stacked in matrix $\boldsymbol{Y}_b$ as: $\boldsymbol{Y}_b = \begin{bmatrix} m_1 \\ m_2 \\ m_3 \\ \vdots \\ \vdots \end{bmatrix}$.

The procedure is stopped when the length of the artificial matrix $\boldsymbol{Y}_b$ exhibits a length exceeding T. Observations exceeding T are cut off to ensure that the artificial data matrix $\boldsymbol{Y}_b$ has the same length as the original data matrix $\boldsymbol{Y}$. This process corresponds to one iteration b of the blocks bootstrap procedure. Employing this blocks bootstraps, for each iteration b, the Tx1 vectors,$\boldsymbol{x}_{b,1}$, $\boldsymbol{x}_{b,2}$, …, $\boldsymbol{x}_{b,N}$ are extracted from matrix $\boldsymbol{Y}_b$, and the cutoff estimators are estimated using the procedure described in Sect. 3, giving us: $\begin{bmatrix} \widehat{x}_{MIN,b,1} & \widehat{x}_{MIN,b,2} & \cdots & \widehat{x}_{MIN,b,N} \end{bmatrix}$.

This blocks bootstrap procedure is performed using $b = 1, \ldots, 1000$ iterations and point estimates are stacked into BxN matrix $\widehat{\boldsymbol{x}}_{MIN,BOOT}$: .

$$\widehat{\boldsymbol{x}}_{MIN,BOOT} = \begin{pmatrix} \widehat{x}_{MIN,1,1} & \widehat{x}_{MIN,1,2} & \cdots & \cdots & \widehat{x}_{MIN,1,N} \\ \widehat{x}_{MIN,2,1} & \widehat{x}_{MIN,1,2} & \cdots & \cdots & \widehat{x}_{MIN,2,N} \\ \vdots & \vdots & \vdots & \vdots & \vdots \\ \vdots & \vdots & \vdots & \vdots & \vdots \\ \widehat{x}_{MIN,B,1} & \widehat{x}_{MIN,B,2} & \cdots & \cdots & \widehat{x}_{MIN,B,N} \end{pmatrix}$$

The corresponding bootstrapped standard errors $\widehat{\sigma}_{\widehat{x}_{MIN,BOOT},i}$ are then given by: $\widehat{\sigma}_{\widehat{x}_{MIN,BOOT},i} = \sqrt{\frac{1}{B}\sum_{b=1}^{B}\left(\widehat{x}_{MIN,b,i} - \overline{\widehat{x}}_{MIN,b,i}\right)^2}$.

This table reports the descriptive statistics for the cutoff distributions derived from blocks bootstraps.

$\widehat{x}_{MIN,i}$ stats for $\widehat{\sigma}^2_i$:	$\widehat{\sigma}^2_{AUD/USD}$	$\widehat{\sigma}^2_{CAD/USD}$	$\widehat{\sigma}^2_{CHF/USD}$	$\widehat{\sigma}^2_{EUR/USD}$	$\widehat{\sigma}^2_{GBP/USD}$	$\widehat{\sigma}^2_{JPY/USD}$	$\widehat{\sigma}^2_{NOK/USD}$	$\widehat{\sigma}^2_{NZD/USD}$	$\widehat{\sigma}^2_{SEK/USD}$
Mean	0.0211	0.0093	0.0090	0.0099	0.0116	0.0085	0.0289	0.0193	0.0210
Median	0.0207	0.0085	0.0088	0.0093	0.0114	0.0078	0.0260	0.0193	0.0202
Maximum	0.0501	0.0242	0.0252	0.0261	0.0307	0.0293	0.0725	0.0477	0.0396

Table 4 (continued)

$\widehat{x}_{MIN,i}$ stats for $\widehat{\sigma}^2_i$:	$\widehat{\sigma}^2_{AUD/USD}$	$\widehat{\sigma}^2_{CAD/USD}$	$\widehat{\sigma}^2_{CHF/USD}$	$\widehat{\sigma}^2_{EUR/USD}$	$\widehat{\sigma}^2_{GBP/USD}$	$\widehat{\sigma}^2_{JPY/USD}$	$\widehat{\sigma}^2_{NOK/USD}$	$\widehat{\sigma}^2_{NZD/USD}$	$\widehat{\sigma}^2_{SEK/USD}$
Minimum	0.0079	0.0055	0.0059	0.0054	0.0059	0.0042	0.0094	0.0112	0.0070
Std. Dev	0.0070	0.0024	0.0025	0.0032	0.0032	0.0035	0.0088	0.0039	0.0083
Skewness	0.4849	2.0567	3.0587	2.2642	0.9492	3.5718	1.2050	1.9111	−0.0170
Kurtosis	4.3240	9.8631	15.2831	10.0170	5.0269	17.1929	5.0485	14.0240	1.7157
Jarque–Bera (JB)	112.23	2667.61	7845.75	2906.07	321.34	10519.58	416.86	5672.40	68.77
p-value (JB)	0.0000	0.0000	0.0000	0.0000	0.0000	0.0000	0.0000	0.0000	0.0000
Observations	1000	1000	1000	1000	1000	1000	1000	1000	1000

Table 5 Correlation matrix for power-law exponents

We implement a blocks bootstrap procedure, as proposed in Grobys (2024). Denoting the selected block length as m, a blocks bootstrap procedure is chosen such that $E[m] = \sqrt{T}$. Then the Tx1 data vectors of FX variances $i = 1, \ldots, N$, denoted as $\boldsymbol{x}_i$, are stacked into matrix $\boldsymbol{Y}$: $\boldsymbol{Y} = [\boldsymbol{x}_1, \boldsymbol{x}_2, \ldots, \boldsymbol{x}_N]$.

The blocks of the dimension *m*xK are randomly drawn from matrix $\boldsymbol{Y}$ with respect to the time dimension $t = 1, \ldots, T$. These blocks are governed by a geometric distribution—that is, $m \sim GEO(p)$ with $E[m] = \frac{(1-p)}{p}$. Drawing geometrically-distributed random blocks ensures that the variance data are stationarity (Godfrey, 2009). Since our data has a length of 2383 implying $\sqrt{T} \approx 49$, we use $E[m] = 49, p = 0.0200$. Note that the blocks drawn from $\boldsymbol{Y}$ vary in lengths. The randomly drawn blocks, m, which have dimensions *m*xK from data matrix $\boldsymbol{Y}$, are stacked in matrix $\boldsymbol{Y}_b$ as: $\boldsymbol{Y}_b = \begin{bmatrix} m_1 \\ m_2 \\ m_3 \\ \vdots \end{bmatrix}$.

The procedure is stopped when the length of the artificial matrix $\boldsymbol{Y}_b$ exhibits a length exceeding *T*. Observations exceeding *T* are cut off to ensure that the artificial data matrix $\boldsymbol{Y}_b$ has the same length as the original data matrix $\boldsymbol{Y}$. This process corresponds to one iteration b of the blocks bootstrap procedure. Employing this blocks bootstraps, for each iteration b, the Tx1 vectors,$\boldsymbol{x}_{b,1}$, $\boldsymbol{x}_{b,2}$, …, $\boldsymbol{x}_{b,N}$ are extracted from matrix $\boldsymbol{Y}_b$, and the MLE estimators for power-law exponents are estimated using the procedure described in the previous section giving us: $\begin{bmatrix} \widehat{\alpha}_{b,1} & \widehat{\alpha}_{b,2} & \cdots & \widehat{\alpha}_{b,N} \end{bmatrix}$.

This blocks bootstrap procedure is performed using $b = 1, \ldots, 1000$ iterations and point estimates are stacked into BxN matrices $\widehat{\boldsymbol{\alpha}}_{BOOT}$

:
$$\widehat{\boldsymbol{\alpha}}_{BOOT} = \begin{pmatrix} \widehat{\alpha}_{1,1} & \widehat{\alpha}_{1,2} & \cdots & \cdots & \widehat{\alpha}_{1,N} \\ \widehat{\alpha}_{2,1} & \widehat{\alpha}_{1,2} & \cdots & \cdots & \widehat{\alpha}_{2,N} \\ \vdots & \vdots & \vdots & \vdots & \vdots \\ \vdots & \vdots & \vdots & \vdots & \vdots \\ \widehat{\alpha}_{B,1} & \widehat{\alpha}_{B,2} & \cdots & \cdots & \widehat{\alpha}_{B,N} \end{pmatrix}.$$

Since this blocks bootstrap approach retains co-dependencies across the data, it enables us to compute the following covariances using the matrices $\widehat{\boldsymbol{\alpha}}_{BOOT}$: $\widehat{\sigma}_{\widehat{\alpha}_{BOOT},i,j} = \frac{1}{B}\sum_{b=1}^{B}\left(\widehat{\alpha}_{b,i} - \overline{\widehat{\alpha}}_{b,i}\right)\left(\widehat{\alpha}_{b,j} - \overline{\widehat{\alpha}}_{b,j}\right)$ with $i \neq j$,

for $i, j = 1, \ldots, N$. The corresponding NxN covariance matrices is denoted as $COV(\widehat{\boldsymbol{\alpha}}_{BOOT})$. This table reports the corresponding correlation matrix for power-law exponents

Table 5 (continued)

Correlation matrix for power-law exponents									
$\widehat{\alpha}$ for $\widehat{\sigma}_i^2$: (*t*-statistic)	$\widehat{\sigma}^2_{AUD/USD}$	$\widehat{\sigma}^2_{CAD/USD}$	$\widehat{\sigma}^2_{CHF/USD}$	$\widehat{\sigma}^2_{EUR/USD}$	$\widehat{\sigma}^2_{GBP/USD}$	$\widehat{\sigma}^2_{JPY/USD}$	$\widehat{\sigma}^2_{NOK/USD}$	$\widehat{\sigma}^2_{NZD/USD}$	$\widehat{\sigma}^2_{SEK/USD}$
$\widehat{\sigma}^2_{AUD/USD}$	1								
	(—)								
$\widehat{\sigma}^2_{CAD/USD}$	0.52***	1							
	(19.36)	(—)							
$\widehat{\sigma}^2_{CHF/USD}$	0.22***	0.22***	1						
	(7.27)	(7.03)	(—)						
$\widehat{\sigma}^2_{EUR/USD}$	0.18***	0.19***	0.42***	1					
	(5.84)	(6.24)	(14.78)	(—)					
$\widehat{\sigma}^2_{GBP/USD}$	0.46***	0.48***	0.26***	0.22***	1				
	(16.19)	(17.50)	(8.64)	(6.99)	(—)				
$\widehat{\sigma}^2_{JPY/USD}$	0.33***	0.39***	0.23***	0.15***	0.48***	1			
	(10.90)	(13.32)	(7.64)	(4.81)	(17.33)	—			
$\widehat{\sigma}^2_{NOK/USD}$	0.60***	0.49***	0.26***	0.17***	0.43***	0.27***	1		
	(23.53)	(17.64)	(8.51)	(5.30)	(14.97)	(8.86)	(—)		
$\widehat{\sigma}^2_{NZD/USD}$	0.59***	0.54***	0.39***	0.28***	0.64***	0.42***	0.59***	1	
	(23.33)	(20.26)	(13.48)	(9.09)	(26.47)	(14.73)	(22.99)	(—)	
$\widehat{\sigma}^2_{SEK/USD}$	0.21***	0.14***	0.10***	0.14***	0.24***	0.10***	0.17***	0.23***	1
	(6.64)	(4.36)	(3.28)	(4.37)	(7.85)	(3.12)	(5.55)	(7.55)	(—)

***Statistically significant on a 1% level

Table 6 Testing for a common power-law exponent
To explore whether a common component governing power-law behavior of FX variances exists, the following test statistic is proposed: $\widehat{\lambda} = (\dot{\boldsymbol{\alpha}} - q1)\prime \widehat{\boldsymbol{\Sigma}}_{\widehat{\boldsymbol{\alpha}}}^{-1} (\dot{\boldsymbol{\alpha}} - q1)$,
where the covariance matrix $\widehat{\boldsymbol{\Sigma}}_{\widehat{\boldsymbol{\alpha}}} = COV(\widehat{\boldsymbol{\alpha}}_{BOOT})$, has the dimension NxN, $\dot{\boldsymbol{\alpha}}$ is a Nx1 vector of the unbiased estimated power-law exponents, 1 is a Nx1 vector consisting of ones, and q is the hypothesized common power-law exponent. The estimated test statistic denoted as $\widehat{\lambda}$ is under the null hypothesis distributed as $\chi^2(N)$. The test statistic is iteratively estimated covering the economically important interval $q = (2.1, 2.2, \ldots, 3.1)$. Since power-law exponents for nine FX variances are tested, the corresponding test statistic is under the null hypothesis distributed as $\chi^2(9)$. Using a statistical significance level of 5% level, the null hypothesis is not rejected for $\widehat{\lambda} < 16.92$. Bold figures indicate statistical significance on a 5% level

q	$\widehat{\lambda}$
2.1	**37.17**
2.2	**29.48**
2.3	**23.26**
2.4	**18.53**
2.5	15.29
2.6	13.53
2.7	13.26
2.8	14.47
2.9	**17.17**
3.0	**21.36**
3.1	**27.03**

nents is reported in Table 5. We see from Table 5 that all correlations are statistically significant on a 1% level. Whereas correlations between power-law exponents range between 0.10 and 0.64, the average correlation of the correlation matrix is 0.33 suggesting a moderate level of correlation. Furthermore, we implement the test statistic $\widehat{\lambda}$, as described in Section 3.1.4., using $\widehat{\boldsymbol{\Sigma}}_{\widehat{\boldsymbol{\alpha}}} = COV(\widehat{\boldsymbol{\alpha}}_{BOOT})$, and for $\dot{\boldsymbol{\alpha}}$, we employ the mean values of blocks bootstrapped point estimates, as reported in Table 3. As pointed out in Section 3.1.4., the test statistic $\widehat{\lambda}$ is iteratively estimated on the economically important interval $q = (2.1, 2.2, \ldots, 3.1)$. The test statistic is under the null hypothesis distributed as $\chi^2(9)$.

Using a statistical significance level of 5% level, the null hypothesis is not rejected for $\widehat{\lambda} < 16.92$. The results are reported in Table 6. From Table 6 we observe that the null hypothesis cannot be rejected for the interval $2.5 \leq \alpha^* \leq 2.8$. The test statistic $\widehat{\lambda}$ reaches its minimum value for $\alpha^* \approx 2.7$ (p-value 0.1512) which confirms Grobys (2024) who documents a cross-sectional power-law exponent of $\alpha^* \approx 2.6$ that would govern FX risk. Note from Table 6 that the estimated test statistic $\widehat{\lambda}$ is virtually the same for $\alpha^* = 2.6$ and $\alpha^* = 2.7$ despite of (a) our sample being considerably shorter than the one used in Grobys (2024), and despite of (b) using a different FX data provider than the one used in Grobys (2024), suggesting that Grobys' (2024) findings are scientifically replicable.

A common exponent does not necessarily suggest that the power-law function is the same across FX variances. As pointed out in Lux (2000), due to the MLE

approach, estimated power-law exponents depend on the chosen cutoff. Therefore, a question that arises is whether power-law functions governing FX risk exhibit the same cutoff. To explore this issue, we make use of blocks bootstraps and compute the covariance matrix using $E[m] = 49$, and $p = 0.0200$ as in the previous analysis. The estimated correlation matrix for cutoffs is reported in Table 7. From Table 7 we observe that whereas correlations between cutoffs range between −0.03 and 0.24, the average correlation of the correlation matrix is 0.10 suggesting a relatively low level of correlation. Yet, it is important to note that the vast majority of correlations (viz. 24-out-of-36) are statistically significant on a 1% level.

Next, we implement the test statistic $\widehat{\lambda}$, as described in Section 3.1.5., using $\widehat{\boldsymbol{\Sigma}}_{\widehat{\boldsymbol{x}}_{MIN}} = COV(\widehat{\boldsymbol{x}}_{MIN,BOOT})$, and for $\dot{\boldsymbol{x}}$, we employ the mean values of blocks bootstrapped point estimates, as reported in Table 4. As mentioned earlier, the test statistic $\widehat{\lambda}$ is iteratively estimated on the economically on the interval $q = (0.0070, 0.0080, \ldots, 0.0340, 0.0350)$. The test statistic is under the null hypothesis distributed as $\chi^2(9)$. Using a statistical significance level of 5% level, the null hypothesis is not rejected for $\widehat{\lambda} < 16.92$. The results are reported in Table 8. Strikingly, from Table 8 we observe that the null hypothesis cannot be rejected for the interval $0.0090 \leq x^*_{MIN} \leq 0.0130$. Furthermore, the test statistic $\widehat{\lambda}$ reaches its minimum value for $x^*_{MIN} = 0.0100$ (p-value 0.1791). This result suggests that the power-law function governing FX variances indeed exhibit a common cutoff resulting in the universal power law, $p(x) \approx (6.77E-04)x^{-2.7}$ that governs the cross section of realized FX variances.

4.2 Additional Results

Given that the Governing Board of the Swiss National Bank (SNB) decided to discontinue the minimum exchange rate of CHF 1.20 per euro on January 15, 2015, it is surprising to note that our point estimate for α for $\widehat{\sigma}^2_{CHF/USD,t}$ is virtually the same as documented in Grobys' (2023) study using a sample covering the May, 16, 2006 to November 19, 2021 period. Specifically, whereas our point estimate is $\widehat{\alpha} = 2.7798$ (Table 2), Grobys (2023) documented a point estimate of $\widehat{\alpha} = 2.7785$ (see Table 2 in Grobys, 2023). Statistically, these estimates are not different from each other. Therefore, we perform a robustness check by expanding the sample to the overall sample period from January, 2, 2001 to May, 4, 2024, incorporating 6044 daily observations. We replicate all Tables for the expanded sample. The results are reported in Tables 10—17 in the appendix. Overall, the results from our robustness check support our main findings; that is, annualized daily realized FX variances are governed by power laws that do not only exhibit a universal exponent, but also a universal cutoff.

It is interesting to note that using the expanded sample, the power-law null model cannot be rejected for eight-out-of-nine FX variances with p-values derived from Clauset et al.'s (2009) GoF test varying between 0.2660—0.8340 (Table 11).[8] That

[8] Note that we, again, employ 500 iterations for implementing Clauset et al.'s (2009) GoF test.

Table 7 Correlation matrix for cutoffs of estimated power-law functions

We implement a blocks bootstrap procedure, as proposed in Grobys (2024). Denoting the selected block length as m, a blocks bootstrap procedure is chosen such that $E[m] = \sqrt{T}$. Then the Tx1 data vectors of FX variances $i = 1, \ldots, N$, denoted as $\boldsymbol{x}_i$, are stacked into matrix $\boldsymbol{Y}$: $\boldsymbol{Y} = [\boldsymbol{x}_1, \boldsymbol{x}_2, \ldots, \boldsymbol{x}_N]$.

The blocks of the dimension *m*xK are randomly drawn from matrix $\boldsymbol{Y}$ with respect to the time dimension $t = 1, \ldots, T$. These blocks are governed by a geometric distribution—that is, $m \sim GEO(p)$ with $E[m] = \frac{(1-p)}{p}$. Drawing geometrically-distributed random blocks ensures that the variance data are stationarity (Godfrey, 2009). Since our data has a length of 2383 implying $\sqrt{T} \approx 49$, we use $E[m] = 49, p = 0.0200$. Note that the blocks drawn from $\boldsymbol{Y}$ vary in lengths. The randomly drawn blocks, m, which have dimensions *m*xK from data matrix $\boldsymbol{Y}$, are stacked in matrix $\boldsymbol{Y}_b$ as: $\boldsymbol{Y}_b = \begin{bmatrix} m_1 \\ m_2 \\ m_3 \\ \vdots \end{bmatrix}$.

The procedure is stopped when the length of the artificial matrix $\boldsymbol{Y}_b$ exhibits a length exceeding T. Observations exceeding T are cut off to ensure that the artificial data matrix $\boldsymbol{Y}_b$ has the same length as the original data matrix $\boldsymbol{Y}$. This process corresponds to one iteration b of the blocks bootstrap procedure. Employing this blocks bootstraps, for each iteration b, the Tx1 vectors,$\boldsymbol{x}_{b,1}$, $\boldsymbol{x}_{b,2}$, …, $\boldsymbol{x}_{b,N}$ are extracted from matrix $\boldsymbol{Y}_b$, and the cutoffs for power-law functions are estimated using the procedure described in the previous section giving us: $\begin{bmatrix} \widehat{x}_{MIN,b,1} & \widehat{x}_{MIN,b,2} & \cdots & \widehat{x}_{MIN,b,N} \end{bmatrix}$.

This blocks bootstrap procedure is performed using $b = 1, \ldots, 1000$ iterations and point estimates are stacked into BxN matrices $\widehat{\boldsymbol{\alpha}}_{BOOT}$:

$$\widehat{\boldsymbol{x}}_{MIN,BOOT} = \begin{pmatrix} \widehat{x}_{MIN,1,1} & \widehat{x}_{MIN,1,2} & \cdots & \cdots & \widehat{x}_{MIN,1,N} \\ \widehat{x}_{MIN,2,1} & \widehat{x}_{MIN,1,2} & \cdots & \cdots & \widehat{x}_{MIN,2,N} \\ \vdots & \vdots & \vdots & \vdots & \vdots \\ \vdots & \vdots & \vdots & \vdots & \vdots \\ \widehat{x}_{MIN,B,1} & \widehat{x}_{MIN,B,2} & \cdots & \cdots & \widehat{x}_{MIN,B,N} \end{pmatrix}.$$

Since this blocks bootstrap approach retains co-dependencies across the data, it enables us to compute the following covariances using the matrix $\widehat{\boldsymbol{x}}_{MIN,BOOT}$: $\widehat{\sigma}_{\widehat{x}_{MIN,BOOT},i,j} = \frac{1}{B}\sum_{b=1}^{B}\left(\widehat{x}_{MIN,b,i} - \overline{\widehat{x}}_{MIN,b,i}\right)\left(\widehat{x}_{MIN,b,j} - \overline{\widehat{x}}_{MIN,b,j}\right)$ with $i \neq j$,

for $i, j = 1, \ldots, N$. The corresponding NxN covariance matrices is denoted as $COV(\widehat{\boldsymbol{x}}_{MIN,BOOT})$. This table reports the corresponding correlation matrix for cutoffs of power-law functions

Table 7 (continued)

Correlation matrix for cutoffs									
$\widehat{x}_{MIN}$ for $\widehat{\sigma}_i^2$: (*t*-statistic)	$\widehat{\sigma}^2_{AUD/USD}$	$\widehat{\sigma}^2_{CAD/USD}$	$\widehat{\sigma}^2_{CHF/USD}$	$\widehat{\sigma}^2_{EUR/USD}$	$\widehat{\sigma}^2_{GBP/USD}$	$\widehat{\sigma}^2_{JPY/USD}$	$\widehat{\sigma}^2_{NOK/USD}$	$\widehat{\sigma}^2_{NZD/USD}$	$\widehat{\sigma}^2_{SEK/USD}$
$\widehat{\sigma}^2_{AUD/USD}$	1								
	(—)								
$\widehat{\sigma}^2_{CAD/USD}$	0.17***	1							
	(5.37)	(—)							
$\widehat{\sigma}^2_{CHF/USD}$	0.18***	−0.01	1						
	(5.83)	(−0.38)	(—)						
$\widehat{\sigma}^2_{EUR/USD}$	0.11***	−0.06*	0.19***	1					
	(3.48)	(−1.76)	(6.08)	(—)					
$\widehat{\sigma}^2_{GBP/USD}$	0.19***	0.09***	0.13***	0.14***	1				
	(6.28)	(2.82)	(4.06)	(4.61)	(—)				
$\widehat{\sigma}^2_{JPY/USD}$	0.08***	0.03	0.12***	0.16***	0.15***	1			
	(2.68)	(1.10)	(3.72)	(5.00)	(4.69)	(—)			
$\widehat{\sigma}^2_{NOK/USD}$	0.23***	0.06**	0.10***	0.08**	0.14***	0.07**	1		
	(7.58)	(2.05)	(3.10)	(2.49)	(4.47)	(2.37)	(—)		
$\widehat{\sigma}^2_{NZD/USD}$	0.23***	0.06*	0.11***	0.05	0.14***	0.04	0.24***	1	
	(7.39)	(1.77)	(3.63)	(1.52)	(4.56)	(1.22)	(7.74)	(—)	
$\widehat{\sigma}^2_{SEK/USD}$	0.12***	−0.03	0.09***	0.14***	0.12***	0.01	0.15***	0.05*	1
	(3.96)	(−1.03)	(2.87)	(4.44)	(3.67)	(0.47)	(4.71)	(1.70)	(—)

***Statistically significant on a 1% level **Statistically significant on a 5% level *Statistically significant on a 10% level

Table 8 Testing for a common cutoff of power-law functions
To explore whether the power law functions governing realized FX variances exhibit a common cutoff the following test statistic is proposed: $\widehat{\lambda} = (\dot{\boldsymbol{x}}_{MIN} - r1)' \widehat{\boldsymbol{\Sigma}}^{-1}_{\widehat{\boldsymbol{x}}_{MIN}} (\dot{\boldsymbol{x}}_{MIN} - r1)$, where the covariance matrix $\widehat{\boldsymbol{\Sigma}}_{\widehat{\boldsymbol{x}}_{MIN}} = COV(\widehat{\boldsymbol{x}}_{MIN,BOOT})$, has the dimension NxN, $\dot{\boldsymbol{x}}_{MIN}$ is a Nx1 vector of unbiased estimated cutoffs, 1 is a Nx1 vector consisting of ones, and r is the hypothesized common cutoff. The estimated test statistic denoted as $\widehat{\lambda}$ is under the null hypothesis distributed as $\chi^2(N)$. The test statistic is iteratively estimated covering the full range of the vector $\widehat{\boldsymbol{x}}_{MIN}$, that is, the hypothesis tests are implemented on the interval $r = (0.007,0.008,0.009,\ldots,0.034,0.035)$. Since cutoffs for nine FX variances are tested, the corresponding test statistic is under the null hypothesis distributed as $\chi^2(9)$. Using a statistical significance level of 5% level, the null hypothesis is not rejected for $\widehat{\lambda} < 16.92$. Bold figures indicate statistical significance on a 5% level

q	$\widehat{\lambda}$
0.0070	**17.68**
0.0080	**15.00**
0.0090	13.33
0.0100	12.65
0.0110	12.99
0.0120	14.33
0.0130	16.67
0.0140	**20.03**
0.0150	**24.38**
0.0160	**29.74**
0.0170	**36.11**
0.0180	**43.48**
0.0190	**51.86**
0.0200	**61.24**
0.0210	**71.63**
0.0220	**83.02**
0.0230	**95.42**
0.0240	**108.82**
0.0250	**123.23**
0.0260	**138.65**
0.0270	**155.07**
0.0280	**172.49**
0.0290	**190.92**
0.0300	**210.36**
0.0310	**230.80**
0.0320	**252.24**
0.0330	**155.07**
0.0340	**172.49**
0.0350	**190.92**

means using more data, the power-law models appear to provide a better fit. This should not come as a great surprise because Taleb (2010) noted that it requires a large data set so that fractal properties can be ascertained in data because low-probability events are per definition rare. Next, the correlation matrix of power-law exponent exhibits an average correlation of $\overline{\rho} = 0.49$ (Table 14) which is considerably higher than the average correlation of power-law exponents conditioned on the subsam-

ple used for the main analysis. However, the average correlation of the correlation matrix for cutoffs (Table 16) is as low as the figure reported in the main analysis (e.g. $\overline{\rho} = 0.10$).

Interestingly, using the expanded sample, the optimal cross-sectional power-law exponent is estimated at $\alpha^* \approx 2.9$ with corresponding p-value of 0.1188 (Table 15). However, there are at least two interesting results worth noting: First, Table 11 shows that the null hypothesis $\alpha^* = 2.7$ cannot be rejected (p-value 0.05670), whereas the null hypothesis $\alpha^* = 3.1$ is clearly rejected (p-value 0.0329). As a consequence, the results derived from the expanded sample support earlier evidence that the common cross-sectional power-law exponent must be $\alpha^* \leq 3.0$ implying that the variance of realized FX variance is undefined.

Furthermore, testing whether the power-law functions of FX variances exhibit a common cutoff, the results reported in Table 17 indeed provide evidence for that the null hypothesis of a common cutoff cannot be rejected for the interval $0.0150 \leq x^*_{MIN} \leq 0.0220$. The test statistic $\widehat{\lambda}$ reaches its minimum value for $x^*_{MIN} = 0.0190$ (p-value 0.2202). While this result confirms the hypothesized common cutoff for power-law function of FX variances, the optimum is in its economic magnitude statistically significantly higher than reported in the main analysis (e.g., $x^*_{MIN} = 0.0100$). A potential reason for this issue could be an adaption of emergent market behavior that facilitates that power-law behavior of FX variances experience a lower threshold. This effect becomes evident when comparing the percentages of power-law observations from the main sample with the expanded sample: For most FX variance distributions, the percentage of power-law observations is higher for the sample from January, 16, 2015 to May, 4, 2024 as opposed to the overall sample from January, 2, 2001 to May, 4, 2024.

Finally, a reader could be concerned about the importance of the covariance matrix when implementing joint test for analyzing whether a common cutoff for power-law functions exists. Admittedly, the average correlation for $\widehat{\mathbf{\Sigma}}_{\widehat{\boldsymbol{x}}_{MIN}}$ is considerably smaller than for $\widehat{\mathbf{\Sigma}}_{\widehat{\boldsymbol{\alpha}}}$, regardless the sample. To address this concern, we implement a test where we assume $COV\left(\widehat{x}_{MIN,i}, \widehat{x}_{MIN,j}\right) = 0 \forall i \neq j$, $\widehat{\mathbf{\Sigma}}_{\widehat{\boldsymbol{x}}_{MIN}}$ giving us:

$$\widehat{\mathbf{\Sigma}}_{\widehat{\boldsymbol{x}}_{MIN}} = \begin{pmatrix} \widehat{\sigma}^2_{\widehat{x}_{MIN,BOOT,1}} & 0 & \cdots & 0 \\ 0 & \widehat{\sigma}^2_{\widehat{x}_{MIN,BOOT,2}} & \cdots & 0 \\ 0 & 0 & \ddots & 0 \\ 0 & \cdots & 0 & \widehat{\sigma}^2_{\widehat{x}_{MIN,BOOT,N}} \end{pmatrix}.$$

Using this covariance matrix, we again make use of the test specified in Eq. (9). The results using data on the main sample (January, 16, 2015 to May, 4, 2024) are reported in Table 18. In line with Table 8, we observe from Table 18 that we cannot reject the null hypothesis that a common cutoff exists. However, we observe that disregarding from covariances, the optimum is estimated at $x^*_{MIN} = 0.0110$ (p-value 0.1220). On the other hand, a hypothesized optimum of $x^*_{MIN} = 0.0100$, as suggested from the main analysis, cannot be rejected either (p-value 0.0843). Overall, even if we

disregard from covariances between cutoffs, we cannot reject the hypothesis that a common cutoff exist that governs the universal power-law function for FX variances.

5 Discussion

5.1 Alignment with Prior Studies

Recent literature extensively examines the power-law behavior of realized FX variances. Consistent with Grobys (2023, 2024) and Fathi et al. (2024), the findings of this study indicate that, for the majority of realized FX variances, the estimated power-law exponents (viz., $\widehat{\alpha} \approx 3$) are sufficiently small to cast doubt on the reliability of estimated sample variances. While Grobys (2024) provides evidence for a universal power-law exponent governing the cross-section of realized FX variances, this study posits that the exponent of a power-law function is intrinsically linked to the power-law cutoff. Expanding on Grobys' (2024) work, we investigate whether the universal power-law also exhibits a universal cutoff. By proposing a joint statistical test, the results reveal robust evidence supporting the existence of a universal cutoff. Previous research predominantly focused on analyzing power laws for individual datasets and proposed various methodologies for determining the optimal cutoff for power-law functions (viz., Clauset et al., 2009; Lux, 2000; White et al., 2008). However, these approaches are designed for single datasets, limiting their applicability to broader contexts. The present study extends this body of literature by introducing a statistical test derived from modern blocks bootstrap methods. This innovative procedure enables the estimation of covariance matrices for cutoffs across multiple data series, facilitating robust tests to determine whether multiple datasets conform to power laws with a common cutoff. Additionally, it identifies a potentially optimal universal cutoff by maximizing the associated p-value. By bridging methodological gaps, this study contributes to a more comprehensive understanding of power-law behaviors in FX variance distributions.

5.2 Applications and Implications

5.2.1 Practical Applications of a Universal Power Law in FX Variances

The universal power law governing FX variances has significant implications for various practical applications (viz., risk management, portfolio diversification, algorithmic trading, and regulatory agencies). In the realm of risk management, the power law provides a robust framework for modeling extreme behaviors in variance distributions, enabling institutions to improve volatility forecasting and tail risk estimation. This approach enhances the precision of stress-testing protocols and allows for better allocation of risk capital, mitigating exposure to unpredictable fluctuations. As pointed out in Taleb (2020), traditional finance theory has a preference for parametric, less robust, methods. By aligning risk management practices with the heavy-tailed nature of FX variances, financial institutions can more effectively address severe market shocks. Furthermore, portfolio diversification strategies can also benefit from

insights derived from the universal power law. The commonalities in FX variances' tail behaviors indicate that traditional diversification benefits may be diminished during extreme market events. Understanding these limitations enables investors to design more resilient portfolios and develop hedging strategies that account for the heightened risks associated with correlated extreme events. This refinement in strategy supports improved portfolio performance under stress conditions.

In the domain of algorithmic trading, the universal power law can refine trading algorithms by integrating more accurate models of tail behaviors. These enhanced models improve the identification of abnormal price movements, enabling better execution strategies and reducing slippage. Additionally, incorporating these insights into order-routing systems allows for optimal responses to abrupt volatility spikes, boosting profitability and efficiency in high-frequency trading environments.

From a regulatory perspective, the universal power law offers valuable tools for assessing systemic risks in FX markets. By acknowledging shared tail behaviors across currency pairs, regulators can design preemptive measures to mitigate cascading effects during extreme events. In this regard, Cirillo and Taleb (2020) emphasize that Extreme-Value-Theory-based risk management is compatible with the (non-naïve) precautionary principle and should be the leading driver for policy decisions under jointly systemic and extreme risks. The power law framework also aids in calibrating capital requirements, ensuring institutions are adequately prepared for rare but severe market shocks. These applications contribute to enhancing the stability and resilience of the global financial system, aligning regulatory policies with empirical market dynamics.

5.2.2 Benefits of Refinements in Methodologies for Modeling FX Variances

The refinements in methodologies for modeling FX variances offer substantial benefits across multiple dimensions, notably accuracy, resilience, and policy and strategy development. These enhancements are critical for aligning analytical frameworks with the empirical realities of financial markets. Accuracy is a primary benefit of these refinements, as they improve the precision of statistical models by incorporating modern techniques such as blocks bootstrap and covariance matrix integration. By accounting for dependencies and cross-sectional correlations in FX variances, these methods mitigate biases introduced by traditional single-equation approaches. This leads to more reliable estimates of key parameters, such as power-law exponents and cutoffs, enabling a deeper understanding of tail behaviors and extreme events in a cross-sectional setting. Enhanced accuracy directly translates into better predictive capabilities for volatility and risk assessments.

Resilience is another critical advantage, as the refined methodologies equip financial institutions to better withstand market shocks. Specifically, tail-focused modeling, for example, emphasizes the statistical significance of rare but impactful events, facilitating robust stress-testing and crisis management frameworks (Taleb, 2020). By focusing on heavy-tailed distributions, institutions can proactively prepare for extreme scenarios, thereby enhancing their operational stability and reducing systemic vulnerabilities in the FX market.

Finally, these refinements provide significant contributions to policy and strategy development. For policymakers, the integration of advanced techniques offers tools for assessing systemic risks and calibrating regulatory measures, such as capital requirements, to address market volatility (Cirillo & Taleb, 2020). For financial practitioners, the improved accuracy and resilience of these models support the design of adaptive investment and hedging strategies that align with real-world dynamics. Together, these benefits bridge theoretical advancements with practical applications, ultimately fostering a more robust and stable financial ecosystem.

6 Conclusion

Recent research provided evidence for that realized FX variances exhibit the same power-law behavior manifested in a common cross-sectional power-law exponent (Grobys, 2024). Using MLE, we argue that the exponent of a power law and the power-law-cutoff are intimately related because the exponent depends on the chosen cutoff. To explore whether a universal cutoff exist, we extend recent research and propose a novel test derived from modern blocks bootstrap. Interestingly, the evidence suggests indeed the presence of such a universal cutoff. Overall, our result suggests that the universal power law governing realized FX variances is characterized by the distribution $p(x) \approx (6.77E-04)x^{-2.7}$. Furthermore, our results imply that for at least five-out-of-nine realized FX variances, the scope of power-law behavior is underestimated. In fact, cutoffs derived from single-equation models suggest for $\widehat{\sigma}^2_{AUD/USD}$, $\widehat{\sigma}^2_{GBP/USD}$, $\widehat{\sigma}^2_{NOK/USD}$, $\widehat{\sigma}^2_{NZD/USD}$, $\widehat{\sigma}^2_{SEK/USD}$, that $\widehat{x}_{MIN} > 0.01$ resulting in that the percentage of sample observations governed by the power law is underestimated. We argue that our results have important implication for FX risk management as they call for refinements in methodologies used to model FX risk.

The findings of the present study, which document that various realized FX variances are governed by a power law with a universal exponent and cutoff, can be supported and explained through the theoretical framework derived in the study of Lux (1995). Specifically, Lux's (1995) work emphasizes that financial markets exhibit non-linear, self-organizing dynamics driven by contagion and herd behavior. These systemic dynamics align with the observed universality of power-law exponents and cutoffs in the present study, suggesting that collective market behavior operates within a predictable threshold before transitioning into extreme variance states. Lux's (1995) discussion of equilibrium states and critical thresholds provides a theoretical basis for understanding the importance of universal cutoffs, which dictate both the range of market behaviors and stability conditions. Furthermore, Lux (1995) highlights how systemic contagion amplifies risk, supporting our assertion that traditional diversification strategies may be less effective under some universal power-law regime. Our methodological approach—such as the use of modern bootstrap techniques— complements Lux's (1995) theoretical insights by empirically validating the universality of power-law properties. Both works underscore the necessity of integrating advanced statistical tools with theoretical models to better understand and predict financial phenomena.

The identification of a common cutoff governing the tail behavior of FX variances has important practical implications for financial risk management. Risk models used for capital allocation, stress testing, or Value-at-Risk (VaR) rely critically on assumptions about the distributional properties of asset returns or variances. If the cutoff separating the tail regime from the bulk of the distribution is misspecified or inconsistently applied across assets, risk measures may substantially under- or overestimate the probability of extreme events. Our findings suggest that using a common, statistically justified cutoff provides a more unified and realistic foundation for modeling extreme variance behavior across currencies. This contributes to better-informed risk assessments in globally diversified FX portfolios, especially in institutions where multiple currency exposures are modeled jointly.

Finally, our study employs the range-based variance estimator proposed by Parkinson (1980) to model realized FX variances. Future research is encouraged to extend our study by using high frequency data to model realized FX variances like in studies of Yi (2020, 2023, 2025).

Appendix 1

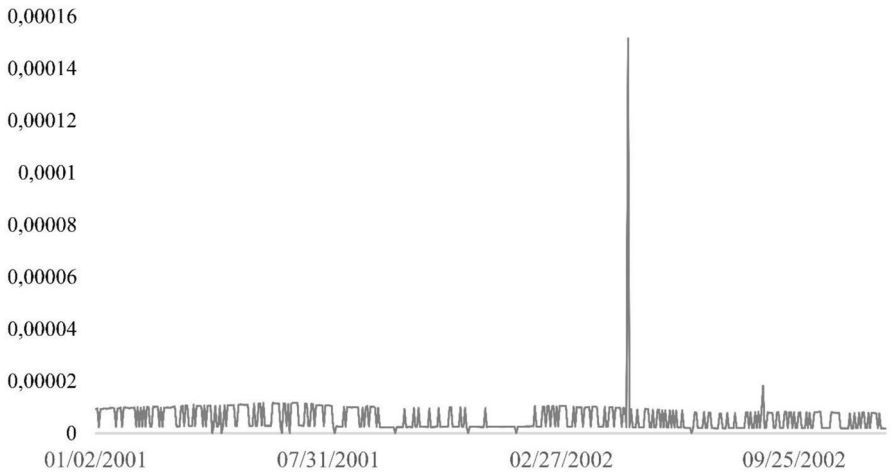

Fig. 1 Evolution of the realized CHF/USD variance for an earlier sample. This figure plots the evolution of the annualized daily CHF/USD variance over the January, 2, 2001 to December, 17, 2002 period

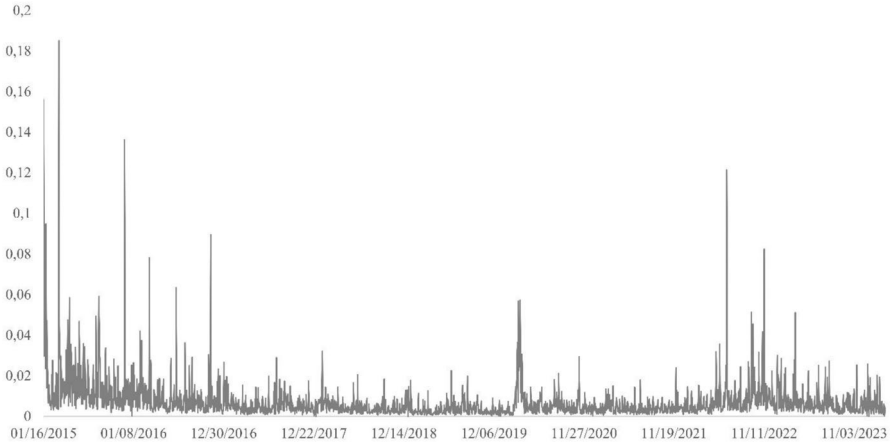

Fig. 2 Evolution of the realized CHF/USD variance for a later sample. This figure plots the evolution of the annualized daily CHF/USD variance over the January, 16, 2015 to March, 4, 2024 period

Table 9 Descriptive statistics of daily CHF/USD variance using the Parkinson-estimator
Publicly available intraday prices for the CHF/USD were downloaded from finance.yahoo.com. The first subsample period is from January, 2, 2001 to December, 17, 2002, the second subsample is from January, 2, 2001 to January, 14, 2015, whereas the third subsample is from January, 16, 2015 to March, 4, 2024. To estimate annualized daily variances, the range-based variance estimator proposed by Parkinson (1980) is employed which is given by: $\sigma_{i,t}^2 = T\frac{1}{4\ln(2)}(\ln(H_{i,t}) - \ln(L_{i,t}))^2$,
where $H_{i,t}$ and $L_{i,t}$ denote the highest and lowest price for foreign exchange rate market i on trading day t, and $\sigma_{i,t}^2$ denotes foreign exchange rate market i's corresponding annualized realized variance where $T = 250$, as 250 trading days per annum are assumed. This table reports the descriptive statistics

	Subsample 1	Subsample 2	Subsample 3
Mean	0.0000	0.0109	0.0071
Median	0.0000	0.0070	0.0044
Maximum	0.0002	0.8345	0.1851
Minimum	0.0000	0.0000	0.0000
Std. Dev	0.0000	0.0209	0.0101
Skewness	14.3814	21.0417	7.4236
Kurtosis	279.1802	723.9203	91.9874
Jarque–Bera (JB)	1,638,435.00	79,528,311.00	808,154.30
(*p*-value JB)	0.0000	0.0000	0.0000
Observations	510	3660	2383

Table 10 Descriptive statistics of daily range-based variances using the Parkinson-estimator over an expanded sample

Publicly available intraday prices for the AUD/USD, CAD/USD, CHF/USD, EUR/USD, GBP/USD, JPY/USD, NOK/USD, NZD/USD, and SEK/USD exchange rates were downloaded from finance.yahoo.com. The sample period is from January, 2, 2001 to May, 4, 2024. Only the intersection of the data is employed; that is, only daily data are accounted for where all FX rates were quoted on the same day, leaving us with 6044 daily observations. To estimate annualized daily variances, the range-based variance estimator proposed by Parkinson (1980) is employed which is given by: $\sigma^2_{i,t} = T\frac{1}{4\ln(2)}(\ln(H_{i,t}) - \ln(L_{i,t}))^2$,

where $H_{i,t}$ and $L_{i,t}$ denote the highest and lowest price for foreign exchange rate market i on trading day t, and $\sigma^2_{i,t}$ denotes foreign exchange rate market i's corresponding annualized realized variance where $T = 250$, as 250 trading days per annum are assumed. This table reports the descriptive statistics

	AUD/USD	CAD/USD	CHF/USD	EUR/USD	GBP/USD	JPY/USD	NOK/USD	NZD/USD	SEK/USD
Mean	0.0161	0.0077	0.0109	0.0088	0.0091	0.0099	0.0165	0.0173	0.0150
Median	0.0090	0.0047	0.0057	0.0055	0.0053	0.0056	0.0096	0.0107	0.0093
Maximum	1.0733	0.3174	9.0723	0.1977	1.4589	0.5085	0.9426	0.6342	0.5904
Minimum	0.0000	0.0000	0.0000	0.0000	0.0000	0.0000	0.0000	0.0000	0.0000
Std. Dev	0.0355	0.0114	0.1179	0.0112	0.0257	0.0188	0.0311	0.0262	0.0213
Skewness	15.5659	9.2531	75.2216	5.3765	37.3225	12.9020	13.2053	9.3422	7.0952
Kurtosis	358.7445	174.4223	5777.0300	53.0992	1897.7740	267.1703	304.2357	151.0899	117.7654
Jarque–Bera (JB)	32114632.00	7486525.00	8400000000.00	661202.80	906000000.00	17742113.00	23027762.00	5610773.00	3367633.00
(p-value JB)	0.0000	0.0000	0.0000	0.0000	0.0000	0.0000	0.0000	0.0000	0.0000
Observations	6044	6044	6044	6044	6044	6044	6044	6044	6044

Table 11 Estimated power-law functions for daily FX variances over an expanded sample

Daily FX variances are modeled using the following power-law function: $p\left(x\right)=Cx^{-\alpha}$,
where $C=\left(\alpha-1\right)x_{MIN}^{\alpha-1}$ with $\alpha\in\{\mathbb{R}_{+}\left|\alpha>1\right.\}$, x denotes the respective annualized daily or weekly FX variance provided $x\in\{\mathbb{R}_{+}\left|x_{MIN}\leq x<\infty\right.\}$, x_{MIN} is the minimum value governed by the power-law process, and α is the magnitude of the corresponding tail exponent. The power-law exponents are estimated as: $\widehat{\alpha}=1+N\left(\sum_{i=1}^{N}\ln\left(\frac{x_i}{x_{MIN}}\right)\right)^{-1}$,
where $\widehat{\alpha}$ denotes the MLE estimator, N is the number of observations exceeding x_{MIN}, and other notations are as previously defined. The estimate $\widehat{\alpha}$ is selected based on the optimal Kolmogorov–Smirnov (KS) distance D measuring the maximum distance between the cumulative density functions (CDFs) of the data and the fitted power-law model as defined by: $D=MAX_{x\geq x_{MIN}}\left|S\left(x\right)-P(x)\right|$,
where $S\left(x\right)$ is the CDF of the data for the observation with a value of at least x_{MIN}, and $P(x)$ is the CDF for the power-law model that best fits the data in the region $x\geq x_{MIN}$. Estimate $\widehat{x}_{MIN}$ is then the value of x_{MIN} that minimizes D. This table reports the estimates $\widehat{\alpha}$, $\widehat{x}_{min}$, $\widehat{\sigma}$, and N for daily FX variance data. Also, the p-values for goodness-of-fit (GoF) tests are reported that test estimated power-law models under the null hypotheses. The sample period is from January, 2, 2001 to May, 4, 2024, comprising 6044 daily observations

	$\widehat{\sigma}^2_{AUD/USD}$	$\widehat{\sigma}^2_{CAD/USD}$	$\widehat{\sigma}^2_{CHF/USD}$	$\widehat{\sigma}^2_{EUR/USD}$	$\widehat{\sigma}^2_{GBP/USD}$	$\widehat{\sigma}^2_{JPY/USD}$	$\widehat{\sigma}^2_{NOK/USD}$	$\widehat{\sigma}^2_{NZD/USD}$	$\widehat{\sigma}^2_{SEK/USD}$
$\widehat{\alpha}$	2.6774	3.2201	3.1723	3.3451	2.7394	2.8323	3.1071	3.0547	2.6178
$\widehat{x}_{min}$	0.0236	0.0205	0.0205	0.0228	0.0122	0.0191	0.0541	0.0413	0.0163
$\widehat{\sigma}$	0.0563	0.1102	0.0887	0.1164	0.0538	0.0728	0.1272	0.0991	0.0402
N	923	424	622	423	1082	661	290	450	1670
(N in %)	(15.27%)	(7.02%)	(10.29%)	(7.00%)	(17.90%)	(10.94%)	(4.80%)	(7.45%)	(27.63%)
p-value (GoF)	0.2660	0.5400	0.6540	0.6360	0.7380	0.6020	0.8340	0.4200	0.0000

Table 12 Descriptive statistics of power-law exponent distributions derived from blocks bootstraps for an expanded sample

We implement a blocks bootstrap procedure, as proposed in Grobys (2024). Denoting the selected block length as m, a blocks bootstrap procedure is chosen such that $E[m] = \sqrt{T}$. Then the Tx1 data vectors of FX variances $i = 1, \ldots, N$, denoted as $\boldsymbol{x}_i$, are stacked into matrix $\boldsymbol{Y}$: $\boldsymbol{Y} = [\boldsymbol{x}_1, \boldsymbol{x}_2, \ldots, \boldsymbol{x}_N]$.

The blocks of the dimension *m*xK are randomly drawn from matrix $\boldsymbol{Y}$ with respect to the time dimension $t = 1, \ldots, T$. These blocks are governed by a geometric distribution—that is, $m \sim GEO(p)$ with $E[m] = \frac{(1-p)}{p}$. Drawing geometrically-distributed random blocks ensures that the variance data are stationarity (Godfrey, 2009). Since our data has a length of 6044 implying $\sqrt{T} \approx 79$, we use $E[m] = 49, p = 0.0127$. Note that the blocks drawn from $\boldsymbol{Y}$ vary in lengths. The randomly drawn blocks, m, which have dimensions *m*xK from data matrix $\boldsymbol{Y}$, are stacked in matrix $\boldsymbol{Y}_b$ as: $\boldsymbol{Y}_b = \begin{bmatrix} m_1 \\ m_2 \\ m_3 \\ \vdots \end{bmatrix}$.

The procedure is stopped when the length of the artificial matrix $\boldsymbol{Y}_b$ exhibits a length exceeding T. Observations exceeding T are cut off to ensure that the artificial data matrix $\boldsymbol{Y}_b$ has the same length as the original data matrix $\boldsymbol{Y}$. This process corresponds to one iteration b of the blocks bootstrap procedure. Employing this blocks bootstraps, for each iteration b, the Tx1 vectors,$\boldsymbol{x}_{b,1}, \boldsymbol{x}_{b,2}, \ldots, \boldsymbol{x}_{b,N}$ are extracted from matrix $\boldsymbol{Y}_b$, and the MLE estimators for power-law exponents are estimated using the procedure described in Sect. 3, giving us: $\begin{bmatrix} \widehat{\alpha}_{b,1} & \widehat{\alpha}_{b,2} & \cdots & \widehat{\alpha}_{b,N} \end{bmatrix}$.

This blocks bootstrap procedure is performed using $b = 1, \ldots, 1000$ iterations and point estimates are stacked into BxN matrix $\widehat{\boldsymbol{\alpha}}_{BOOT}$:

$$\widehat{\boldsymbol{\alpha}}_{BOOT} = \begin{pmatrix} \widehat{\alpha}_{1,1} & \widehat{\alpha}_{1,2} & \cdots & \cdots & \widehat{\alpha}_{1,N} \\ \widehat{\alpha}_{2,1} & \widehat{\alpha}_{1,2} & \cdots & \cdots & \widehat{\alpha}_{2,N} \\ \vdots & \vdots & \vdots & \vdots & \vdots \\ \vdots & \vdots & \vdots & \vdots & \vdots \\ \widehat{\alpha}_{B,1} & \widehat{\alpha}_{B,2} & \cdots & \cdots & \widehat{\alpha}_{B,N} \end{pmatrix}.$$

The corresponding bootstrapped standard errors $\widehat{\sigma}_{\widehat{\alpha}_{BOOT},i}$ are then given by: $\widehat{\sigma}_{\widehat{\alpha}_{BOOT},i} = \sqrt{\frac{1}{B}\sum_{b=1}^{B}\left(\widehat{\alpha}_{b,i} - \overline{\widehat{\alpha}}_{b,i}\right)^2}$.

This table reports the descriptive statistics for the power-law exponent distributions derived from blocks bootstraps

$\widehat{\alpha}$ stats for $\widehat{\sigma}_i^2$:	$\widehat{\sigma}^2_{AUD/USD}$	$\widehat{\sigma}^2_{CAD/USD}$	$\widehat{\sigma}^2_{CHF/USD}$	$\widehat{\sigma}^2_{EUR/USD}$	$\widehat{\sigma}^2_{GBP/USD}$	$\widehat{\sigma}^2_{JPY/USD}$	$\widehat{\sigma}^2_{NOK/USD}$	$\widehat{\sigma}^2_{NZD/USD}$	$\widehat{\sigma}^2_{SEK/USD}$
Mean	2.7920	3.2019	3.2301	3.3774	2.7990	2.8090	3.0558	2.9679	2.9415
Median	2.7243	3.1731	3.1737	3.3711	2.7777	2.8084	3.0288	2.9230	2.7828
Maximum	4.3105	4.8915	5.2984	4.4140	4.0709	3.2873	4.4894	4.3482	5.5615

Table 12 (continued)

$\widehat{\alpha}$ stats for $\widehat{\sigma}_i^2$:	$\widehat{\sigma}^2_{AUD/USD}$	$\widehat{\sigma}^2_{CAD/USD}$	$\widehat{\sigma}^2_{CHF/USD}$	$\widehat{\sigma}^2_{EUR/USD}$	$\widehat{\sigma}^2_{GBP/USD}$	$\widehat{\sigma}^2_{JPY/USD}$	$\widehat{\sigma}^2_{NOK/USD}$	$\widehat{\sigma}^2_{NZD/USD}$	$\widehat{\sigma}^2_{SEK/USD}$
Minimum	2.0380	2.1965	2.6806	2.3241	2.1876	2.3135	2.2194	2.2320	2.1108
Std. Dev	0.3405	0.4481	0.2786	0.2971	0.2669	0.1244	0.3172	0.3053	0.5581
Skewness	0.7126	0.2453	1.4804	0.1777	0.5739	0.0091	0.6791	0.7782	1.2875
Kurtosis	3.2790	2.6784	7.6620	3.1193	3.5667	3.6492	4.0033	3.7795	4.6641
Jarque–Bera (JB)	87.88	14.34	1270.86	5.86	68.27	17.57	118.81	126.25	391.67
p-value (JB)	0.0000	0.0008	0.0000	0.0535	0.0000	0.0002	0.0000	0.0000	0.0000
Observations	1000	1000	1000	1000	1000	1000	1000	1000	1000

Table 13 Descriptive statistics of cutoff distributions derived from blocks bootstraps for an expanded sample

We implement a blocks bootstrap procedure, as proposed in Grobys (2024). Denoting the selected block length as m, a blocks bootstrap procedure is chosen such that $E[m] = \sqrt{T}$. Then the Tx1 data vectors of FX variances $i = 1, \ldots, N$, denoted as $\boldsymbol{x}_i$, are stacked into matrix $\boldsymbol{Y}$: $\boldsymbol{Y} = [\boldsymbol{x}_1, \boldsymbol{x}_2, \ldots, \boldsymbol{x}_N]$.

The blocks of the dimension mxK are randomly drawn from matrix $\boldsymbol{Y}$ with respect to the time dimension $t = 1, \ldots, T$. These blocks are governed by a geometric distribution—that is, $m \sim GEO(p)$ with $E[m] = \frac{(1-p)}{p}$. Drawing geometrically-distributed random blocks ensures that the variance data are stationarity (Godfrey, 2009). Since our data has a length of 6044 implying $\sqrt{T} \approx 79$, we use $E[m] = 49, p = 0.0127$. Note that the blocks drawn from $\boldsymbol{Y}$ vary in lengths. The randomly drawn blocks, m, which have dimensions mxK from data matrix $\boldsymbol{Y}$, are stacked in matrix $\boldsymbol{Y}_b$ as: $\boldsymbol{Y}_b = \begin{bmatrix} m_1 \\ m_2 \\ m_3 \\ \vdots \end{bmatrix}$.

The procedure is stopped when the length of the artificial matrix $\boldsymbol{Y}_b$ exhibits a length exceeding T. Observations exceeding T are cut off to ensure that the artificial data matrix $\boldsymbol{Y}_b$ has the same length as the original data matrix $\boldsymbol{Y}$. This process corresponds to one iteration b of the blocks bootstrap procedure. Employing this blocks bootstraps, for each iteration b, the Tx1 vectors, $\boldsymbol{x}_{b,1}$, $\boldsymbol{x}_{b,2}$, …, $\boldsymbol{x}_{b,N}$ are extracted from matrix $\boldsymbol{Y}_b$, and the cutoff estimators are estimated using the procedure described in Section 3, giving us: $\begin{bmatrix} \widehat{x}_{MIN,b,1} & \widehat{x}_{MIN,b,2} & \cdots & \widehat{x}_{MIN,b,N} \end{bmatrix}$.

This blocks bootstrap procedure is performed using $b = 1, \ldots, 1000$ iterations and point estimates are stacked into BxN matrix $\widehat{\boldsymbol{x}}_{MIN,BOOT}$:

$$\widehat{\boldsymbol{x}}_{MIN,BOOT} = \begin{pmatrix} \widehat{x}_{MIN,1,1} & \widehat{x}_{MIN,1,2} & \cdots & \cdots & \widehat{x}_{MIN,1,N} \\ \widehat{x}_{MIN,2,1} & \widehat{x}_{MIN,1,2} & \cdots & \cdots & \widehat{x}_{MIN,2,N} \\ \vdots & \vdots & \vdots & \vdots & \vdots \\ \vdots & \vdots & \vdots & \vdots & \vdots \\ \widehat{x}_{MIN,B,1} & \widehat{x}_{MIN,B,2} & \cdots & \cdots & \widehat{x}_{MIN,B,N} \end{pmatrix}.$$

The corresponding bootstrapped standard errors $\widehat{\sigma}_{\widehat{x}_{MIN,BOOT},i}$ are then given by: $\widehat{\sigma}_{\widehat{x}_{MIN,BOOT},i} = \sqrt{\frac{1}{B}\sum_{b=1}^{B}\left(\widehat{x}_{MIN,b,i} - \overline{\widehat{x}}_{MIN,b,i}\right)^2}$.

This table reports the descriptive statistics for the cutoff distributions derived from blocks bootstraps

$\widehat{x}_{MIN,i}$ stats for $\widehat{\sigma}^2_i$:	$\widehat{\sigma}^2_{AUD/USD}$	$\widehat{\sigma}^2_{CAD/USD}$	$\widehat{\sigma}^2_{CHF/USD}$	$\widehat{\sigma}^2_{EUR/USD}$	$\widehat{\sigma}^2_{GBP/USD}$	$\widehat{\sigma}^2_{JPY/USD}$	$\widehat{\sigma}^2_{NOK/USD}$	$\widehat{\sigma}^2_{NZD/USD}$	$\widehat{\sigma}^2_{SEK/USD}$
Mean	0.0254	0.0181	0.0213	0.0218	0.0130	0.0182	0.0390	0.0313	0.0260
Median	0.0236	0.0205	0.0202	0.0223	0.0122	0.0183	0.0428	0.0255	0.0182
Maximum	0.0892	0.0346	0.0410	0.0387	0.0281	0.0357	0.0916	0.0694	0.1023
Minimum	0.0084	0.0054	0.0126	0.0078	0.0058	0.0082	0.0148	0.0131	0.0102

Table 13 (continued)

$\widehat{x}_{MIN,i}$ stats for $\widehat{\sigma}^2_i$:	$\widehat{\sigma}^2_{AUD/USD}$	$\widehat{\sigma}^2_{CAD/USD}$	$\widehat{\sigma}^2_{CHF/USD}$	$\widehat{\sigma}^2_{EUR/USD}$	$\widehat{\sigma}^2_{GBP/USD}$	$\widehat{\sigma}^2_{JPY/USD}$	$\widehat{\sigma}^2_{NOK/USD}$	$\widehat{\sigma}^2_{NZD/USD}$	$\widehat{\sigma}^2_{SEK/USD}$
Std. Dev	0.0074	0.0062	0.0037	0.0038	0.0033	0.0042	0.0144	0.0114	0.0149
Skewness	1.0736	-0.6936	1.6607	0.0920	1.2657	0.9488	0.4235	0.7626	1.7132
Kurtosis	7.7593	2.1181	6.4980	5.9146	5.2365	4.9287	2.9538	2.7057	6.0311
Jarque–Bera (JB)	1135.90	112.59	969.45	355.37	475.43	305.02	29.97	100.54	871.99
p-value (JB)	0.0000	0.0000	0.0000	0.0000	0.0000	0.0000	0.0000	0.0000	0.0000
Observations	1000	1000	1000	1000	1000	1000	1000	1000	1000

Table 14 Correlation matrix for power-law exponents for an expanded sample

We implement a blocks bootstrap procedure, as proposed in Grobys (2024). Denoting the selected block length as m, a blocks bootstrap procedure is chosen such that $E[m] = \sqrt{T}$. Then the Tx1 data vectors of FX variances $i = 1, \ldots, N$, denoted as $\boldsymbol{x}_i$, are stacked into matrix $\boldsymbol{Y}$: $\boldsymbol{Y} = [\boldsymbol{x}_1, \boldsymbol{x}_2, \ldots, \boldsymbol{x}_N]$.

The blocks of the dimension *m*xK are randomly drawn from matrix $\boldsymbol{Y}$ with respect to the time dimension $t = 1, \ldots, T$. These blocks are governed by a geometric distribution—that is, $m \sim GEO(p)$ with $E[m] = \frac{(1-p)}{p}$. Drawing geometrically-distributed random blocks ensures that the variance data are stationarity (Godfrey, 2009). Since our data has a length of 6044 implying $\sqrt{T} \approx 79$, we use $E[m] = 49, p = 0.0127$. Note that the blocks drawn from $\boldsymbol{Y}$ vary in lengths. The randomly drawn blocks, m, which have dimensions *m*xK from data matrix $\boldsymbol{Y}$, are stacked in matrix $\boldsymbol{Y}_b$ as: $\boldsymbol{Y}_b = \begin{bmatrix} m_1 \\ m_2 \\ m_3 \\ \vdots \end{bmatrix}$.

The procedure is stopped when the length of the artificial matrix $\boldsymbol{Y}_b$ exhibits a length exceeding T. Observations exceeding T are cut off to ensure that the artificial data matrix $\boldsymbol{Y}_b$ has the same length as the original data matrix $\boldsymbol{Y}$. This process corresponds to one iteration b of the blocks bootstrap procedure. Employing this blocks bootstraps, for each iteration b, the Tx1 vectors,$\boldsymbol{x}_{b,1}$, $\boldsymbol{x}_{b,2}$, ..., $\boldsymbol{x}_{b,N}$ are extracted from matrix $\boldsymbol{Y}_b$, and the MLE estimators for power-law exponents are estimated using the procedure described in the previous section giving us: $\begin{bmatrix} \widehat{\alpha}_{b,1} & \widehat{\alpha}_{b,2} & \cdots & \widehat{\alpha}_{b,N} \end{bmatrix}$.

This blocks bootstrap procedure is performed using $b = 1, \ldots, 1000$ iterations and point estimates are stacked into BxN matrices $\widehat{\boldsymbol{\alpha}}_{BOOT}$:

$$\widehat{\boldsymbol{\alpha}}_{BOOT} = \begin{pmatrix} \widehat{\alpha}_{1,1} & \widehat{\alpha}_{1,2} & \cdots & \cdots & \widehat{\alpha}_{1,N} \\ \widehat{\alpha}_{2,1} & \widehat{\alpha}_{1,2} & \cdots & \cdots & \widehat{\alpha}_{2,N} \\ \vdots & \vdots & \vdots & \vdots & \vdots \\ \vdots & \vdots & \vdots & \vdots & \vdots \\ \widehat{\alpha}_{B,1} & \widehat{\alpha}_{B,2} & \cdots & \cdots & \widehat{\alpha}_{B,N} \end{pmatrix}.$$

Since this blocks bootstrap approach retains co-dependencies across the data, it enables us to compute the following covariances using the matrices $\widehat{\boldsymbol{\alpha}}_{BOOT}$: $\widehat{\sigma}_{\widehat{\alpha}_{BOOT},i,j} = \frac{1}{B}\sum_{b=1}^{B}\left(\widehat{\alpha}_{b,i} - \overline{\widehat{\alpha}}_{b,i}\right)\left(\widehat{\alpha}_{b,j} - \overline{\widehat{\alpha}}_{b,j}\right)$ with $i \neq j$,

for $i, j = 1, \ldots, N$. The corresponding NxN covariance matrices is denoted as $COV(\widehat{\boldsymbol{\alpha}}_{BOOT})$. This table reports the corresponding correlation matrix for power-law exponents

Table 14 (continued)

Correlation matrix for power-law exponents of FX variances									
$\widehat{\alpha}$ for $\widehat{\sigma}_i^2$: (*t*-statistic)	$\widehat{\sigma}^2_{AUD/USD}$	$\widehat{\sigma}^2_{CAD/USD}$	$\widehat{\sigma}^2_{CHF/USD}$	$\widehat{\sigma}^2_{EUR/USD}$	$\widehat{\sigma}^2_{GBP/USD}$	$\widehat{\sigma}^2_{JPY/USD}$	$\widehat{\sigma}^2_{NOK/USD}$	$\widehat{\sigma}^2_{NZD/USD}$	$\widehat{\sigma}^2_{SEK/USD}$
$\widehat{\sigma}^2_{AUD/USD}$	1								
	(—)								
$\widehat{\sigma}^2_{CAD/USD}$	0.76***	1							
	(36.63)	(—)							
$\widehat{\sigma}^2_{CHF/USD}$	0.26***	0.24***	1						
	(8.61)	(7.85)	(—)						
$\widehat{\sigma}^2_{EUR/USD}$	0.73***	0.71***	0.21***	1					
	(33.51)	(31.76)	(6.93)	(—)					
$\widehat{\sigma}^2_{GBP/USD}$	0.79***	0.67***	0.36***	0.74***	1				
	(41.36)	(28.20)	(12.33)	(34.38)	(—)				
$\widehat{\sigma}^2_{JPY/USD}$	0.56***	0.53***	0.28***	0.49***	0.55***	1			
	(21.46)	(19.89)	(9.19)	(17.98)	(20.68)	(—)			
$\widehat{\sigma}^2_{NOK/USD}$	0.54***	0.49***	0.08**	0.48***	0.49***	0.31***	1		
	(20.36)	(17.75)	(2.49)	(17.21)	(17.96)	(10.23)	(—)		
$\widehat{\sigma}^2_{NZD/USD}$	0.77***	0.67***	0.23***	0.64***	0.72***	0.52***	0.48***	1	
	(38.40)	(28.32)	(7.62)	(26.11)	(32.50)	(19.20)	(17.31)	(—)	
$\widehat{\sigma}^2_{SEK/USD}$	0.60***	0.53***	0.24***	0.51***	0.58***	0.25***	0.28***	0.45***	1
	(23.39)	(19.96)	(7.70)	(18.82)	(22.40)	(8.14)	(9.07)	(15.96)	(—)

***Statistically significant on a 1% level

Table 15 Testing for a common power-law exponent using an expanded sample
To explore whether a common component governing power-law behavior of FX variances exists, the following test statistic is employed: $\widehat{\lambda} = \left(\widehat{\boldsymbol{\alpha}} - q1\right)' \widehat{\boldsymbol{\Sigma}}_{\widehat{\boldsymbol{\alpha}}}^{-1} \left(\widehat{\boldsymbol{\alpha}} - q1\right)$,
where the covariance matrix $\widehat{\boldsymbol{\Sigma}}_{\widehat{\boldsymbol{\alpha}}} = COV(\widehat{\boldsymbol{\alpha}}_{BOOT})$, has the dimension NxN, $\widehat{\boldsymbol{\alpha}}$ is a Nx1 vector of the estimated power-law exponents, 1 is a Nx1 vector consisting of ones, and q is the hypothesized common power-law exponent. The estimated test statistic, denoted as $\widehat{\lambda}$, is under the null hypothesis distributed as $\chi^2(N)$. The test statistic is iteratively estimated covering the economically important interval $q = (2.1, 2.2, \ldots, 3.1)$. Since power-law exponents for nine FX variances are tested, the corresponding test statistic is under the null hypothesis distributed as $\chi^2(9)$. Using a statistical significance level of 5% level, the null hypothesis is not rejected for $\widehat{\lambda} < 16.92$. Bold figures indicate statistical significance on a 5% level

q	$\widehat{\lambda}$
2.1	**62.80**
2.2	**51.02**
2.3	**40.86**
2.4	**32.33**
2.5	**25.43**
2.6	**20.15**
2.7	16.51
2.8	14.49
2.9	14.10
3.0	15.33
3.1	**18.20**

Table 16 Correlation matrix for cutoffs of estimated power-law functions for an expanded sample

We implement a blocks bootstrap procedure, as proposed in Grobys (2024). Denoting the selected block length as m, a blocks bootstrap procedure is chosen such that $E[m] = \sqrt{T}$. Then the Tx1 data vectors of FX variances $i = 1, \ldots, N$, denoted as $\boldsymbol{x}_i$, are stacked into matrix $\boldsymbol{Y}$: $\boldsymbol{Y} = [\boldsymbol{x}_1, \boldsymbol{x}_2, \ldots, \boldsymbol{x}_N]$.

The blocks of the dimension *m*xK are randomly drawn from matrix $\boldsymbol{Y}$ with respect to the time dimension $t = 1, \ldots, T$. These blocks are governed by a geometric distribution—that is, $m \sim GEO(p)$ with $E[m] = \frac{(1-p)}{p}$. Drawing geometrically-distributed random blocks ensures that the variance data are stationarity (Godfrey, 2009). Since our data has a length of 6044 implying $\sqrt{T} \approx 79$, we use $E[m] = 49, p = 0.0127$. Note that the blocks drawn from $\boldsymbol{Y}$ vary in lengths. The randomly drawn blocks, m, which have dimensions *m*xK from data matrix $\boldsymbol{Y}$, are stacked in matrix $\boldsymbol{Y}_b$ as: $\boldsymbol{Y}_b = \begin{bmatrix} m_1 \\ m_2 \\ m_3 \\ \vdots \end{bmatrix}$.

The procedure is stopped when the length of the artificial matrix $\boldsymbol{Y}_b$ exhibits a length exceeding T. Observations exceeding T are cut off to ensure that the artificial data matrix $\boldsymbol{Y}_b$ has the same length as the original data matrix $\boldsymbol{Y}$. This process corresponds to one iteration b of the blocks bootstrap procedure. Employing this blocks bootstraps, for each iteration b, the Tx1 vectors,$\boldsymbol{x}_{b,1}$, $\boldsymbol{x}_{b,2}$, …, $\boldsymbol{x}_{b,N}$ are extracted from matrix $\boldsymbol{Y}_b$, and the cutoffs for power-law functions are estimated using the procedure described in the previous section giving us: $\begin{bmatrix} \widehat{x}_{MIN,b,1} & \widehat{x}_{MIN,b,2} & \cdots & \widehat{x}_{MIN,b,N} \end{bmatrix}$.

This blocks bootstrap procedure is performed using $b = 1, \ldots, 1000$ iterations and point estimates are stacked into BxN matrices $\widehat{\boldsymbol{\alpha}}_{BOOT}$:

$$\widehat{\boldsymbol{x}}_{MIN,BOOT} = \begin{pmatrix} \widehat{x}_{MIN,1,1} & \widehat{x}_{MIN,1,2} & \cdots & \cdots & \widehat{x}_{MIN,1,N} \\ \widehat{x}_{MIN,2,1} & \widehat{x}_{MIN,1,2} & \cdots & \cdots & \widehat{x}_{MIN,2,N} \\ \vdots & \vdots & \vdots & \vdots & \vdots \\ \vdots & \vdots & \vdots & \vdots & \vdots \\ \widehat{x}_{MIN,B,1} & \widehat{x}_{MIN,B,2} & \cdots & \cdots & \widehat{x}_{MIN,B,N} \end{pmatrix}.$$

Since this blocks bootstrap approach retains co-dependencies across the data, it enables us to compute the following covariances using the matrix $\widehat{\boldsymbol{x}}_{MIN,BOOT}$: $\widehat{\sigma}_{\widehat{x}_{MIN,BOOT},i,j} = \frac{1}{B}\sum_{b=1}^{B}\left(\widehat{x}_{MIN,b,i} - \overline{\widehat{x}}_{MIN,b,i}\right)\left(\widehat{x}_{MIN,b,j} - \overline{\widehat{x}}_{MIN,b,j}\right)$ with $i \neq j$,

for $i, j = 1, \ldots, N$. The corresponding NxN covariance matrices is denoted as $COV(\widehat{\boldsymbol{x}}_{MIN,BOOT})$. This table reports the corresponding correlation matrix for cutoffs of power-law functions

Table 16 (continued)

Correlation matrix for cutoffs associated with power laws of FX variances									
$\widehat{x}_{MIN}$ for $\widehat{\sigma}_i^2$: (*t*-statistic)	$\widehat{\sigma}^2_{AUD/USD}$	$\widehat{\sigma}^2_{CAD/USD}$	$\widehat{\sigma}^2_{CHF/USD}$	$\widehat{\sigma}^2_{EUR/USD}$	$\widehat{\sigma}^2_{GBP/USD}$	$\widehat{\sigma}^2_{JPY/USD}$	$\widehat{\sigma}^2_{NOK/USD}$	$\widehat{\sigma}^2_{NZD/USD}$	$\widehat{\sigma}^2_{SEK/USD}$
$\widehat{\sigma}^2_{AUD/USD}$	1								
	(—-)								
$\widehat{\sigma}^2_{CAD/USD}$	0.35***	1							
	(11.66)	(—-)							
$\widehat{\sigma}^2_{CHF/USD}$	-0.21***	-0.16***	1						
	(-6.78)	(-5.11)	(—-)						
$\widehat{\sigma}^2_{EUR/USD}$	0.24***	0.21***	-0.16***	1					
	(7.76)	(6.84)	(-5.27)	(—-)					
$\widehat{\sigma}^2_{GBP/USD}$	0.41***	0.31***	-0.09***	0.21***	1				
	(14.09)	(10.43)	(-2.82)	(6.84)	(—-)				
$\widehat{\sigma}^2_{JPY/USD}$	0.04	0.10***	0.10***	0.02	-0.01	1			
	(1.11)	(3.04)	(3.28)	(0.63)	(-0.29)	(—-)			
$\widehat{\sigma}^2_{NOK/USD}$	0.20***	0.20***	-0.04	0.21***	0.08**	0.15***	1		
	(6.50)	(6.61)	(-1.32)	(6.86)	(2.53)	(4.86)	(—-)		
$\widehat{\sigma}^2_{NZD/USD}$	0.31***	0.28***	-0.13***	0.16***	0.27***	0.08**	0.18***	1	
	(10.47)	(9.29)	(-4.02)	(5.05)	(8.88)	(2.49)	(5.71)	(—-)	
$\widehat{\sigma}^2_{SEK/USD}$	0.20***	0.22***	-0.10***	0.08***	0.22***	-0.12***	-0.10***	0.00	1
	(6.33)	(7.14)	(-3.15)	(2.59)	(7.12)	(-3.75)	(-3.26)	(0.12)	(—-)

***Statistically significant on a 1% level, **Statistically significant on a 5% level

Table 17 Testing for a common cutoff using an expanded sample
To explore whether the power law functions governing realized FX variances exhibit a common cutoff the following test statistic is employed: $\widehat{\lambda} = \left(\widehat{\boldsymbol{x}}_{MIN} - r1\right)' \widehat{\boldsymbol{\Sigma}}^{-1}_{\widehat{\boldsymbol{x}}_{MIN}} \left(\widehat{\boldsymbol{x}}_{MIN} - r1\right)$, where the covariance matrix $\widehat{\boldsymbol{\Sigma}}_{\widehat{\boldsymbol{x}}_{MIN}} = COV(\widehat{\boldsymbol{x}}_{MIN,BOOT})$, has the dimension NxN, $\widehat{\boldsymbol{x}}_{MIN}$ is a Nx1 vector of the estimated cutoffs, 1 is a Nx1 vector consisting of ones, and r is the hypothesized common cutoff. The estimated test statistic, denoted as $\widehat{\lambda}$, is under the null hypothesis distributed as $\chi^2(N)$. The test statistic is iteratively estimated covering the full range of the vector $\widehat{\boldsymbol{x}}_{MIN}$, that is, the hypothesis tests are implemented on the interval $r = (0.007,0.008,0.009,\ldots,0.034,0.035)$. Since the cutoffs for nine FX variances are tested, the corresponding test statistic is under the null hypothesis distributed as $\chi^2(9)$. Using a statistical significance level of 5% level, the null hypothesis is not rejected for $\widehat{\lambda} < 16.92$. Bold figures indicate statistical significance on a 5% level

q	$\widehat{\lambda}$
0.0070	**49.91**
0.0080	**43.58**
0.0090	**37.82**
0.0100	**32.64**
0.0110	**28.03**
0.0120	**24.00**
0.0130	**20.55**
0.0140	**17.66**
0.0150	15.36
0.0160	13.63
0.0170	12.47
0.0180	11.89
0.0190	11.88
0.0200	12.45
0.0210	13.60
0.0220	15.32
0.0230	**17.61**
0.0240	**20.48**
0.0250	**23.93**
0.0260	**27.95**
0.0270	**32.54**
0.0280	**37.71**
0.0290	**43.46**
0.0300	**49.78**
0.0310	**56.68**
0.0320	**64.15**
0.0330	**72.19**
0.0340	**80.81**
0.0350	**90.01**

Table 18 Testing for a common cutoff under covariance constraints

To explore whether the power law functions governing realized FX variances exhibit a common cutoff the following test statistic is proposed: $\widehat{\lambda} = \left(\widehat{\boldsymbol{x}}_{MIN} - r1\right)' \widehat{\boldsymbol{\Sigma}}^{-1}_{\widehat{\boldsymbol{x}}_{MIN}} \left(\widehat{\boldsymbol{x}}_{MIN} - r1\right)$

where the covariance matrix $\widehat{\boldsymbol{\Sigma}}_{\widehat{\boldsymbol{x}}_{MIN}}$ has the dimension NxN, and because it is assumed here that $COV\left(\widehat{x}_{MIN,i}, \widehat{x}_{MIN,j}\right) = 0 \forall i \neq j$, $\widehat{\boldsymbol{\Sigma}}_{\widehat{\boldsymbol{x}}_{MIN}}$ is a diagonal matrix and defined as:

$$\widehat{\boldsymbol{\Sigma}}_{\widehat{\boldsymbol{x}}_{MIN}} = \begin{pmatrix} \widehat{\sigma}^2_{\widehat{x}_{MIN,BOOT,1}} & 0 & \cdots & 0 \\ 0 & \widehat{\sigma}^2_{\widehat{x}_{MIN,BOOT,2}} & \cdots & 0 \\ & & & 0 \\ 0 & 0 & \ddots & \widehat{\sigma}^2_{\widehat{x}_{MIN,BOOT,N}} \\ 0 & \cdots & 0 & \end{pmatrix}.$$

Furthermore, $\widehat{\boldsymbol{x}}_{MIN}$ is a Nx1 vector of the estimated cutoffs, 1 is a Nx1 vector consisting of ones, and r is the hypothesized common cutoff. The estimated test statistic denoted as $\widehat{\lambda}$ is under the null hypothesis distributed as $\chi^2(N)$. The test statistic is iteratively estimated covering the full range of the vector $\widehat{\boldsymbol{x}}_{MIN}$, that is, the hypothesis tests are implemented on the interval $r = (0.007, 0.008, 0.009, \ldots, 0.034, 0.035)$. Since cutoffs for nine FX variances are tested, the corresponding test statistic is under the null hypothesis distributed as $\chi^2(9)$. Using a statistical significance level of 5% level, the null hypothesis is not rejected for $\widehat{\lambda} < 16.92$. Bold figures indicate statistical significance on a 5% level

q	$\widehat{\lambda}$
0.0070	**27.67**
0.0080	**22.08**
0.0090	**17.94**
0.0100	15.25
0.0110	14.01
0.0120	14.21
0.0130	15.86
0.0140	**18.96**
0.0150	**23.51**
0.0160	**29.51**
0.0170	**36.95**
0.0180	**45.85**

Table 18 (continued)

q	$\widehat{\lambda}$
0.0190	**56.19**
0.0200	**67.98**
0.0210	**81.22**
0.0220	**95.90**
0.0230	**112.04**
0.0240	**129.62**
0.0250	**148.65**
0.0260	**169.13**
0.0270	**191.06**
0.0280	**214.44**
0.0290	**239.26**
0.0300	**265.54**
0.0310	**293.26**
0.0320	**322.43**
0.0330	**353.05**
0.0340	**385.11**
0.0350	**418.63**

A.P. Derivation of the maximum likelihood estimator for the exponent of a power law probability density function.

Let $p(x) = Cx^{-\alpha}$ define the probability density of a power law with cutoff x_{MIN}. The maximum likelihood estimator $\widehat{\alpha}$ is derived as:

$$
\begin{aligned}
&p(x) = Cx^{-\alpha} = (\alpha-1)\, x_{MIN}^{\alpha-1} x^{-\alpha} \\
&\Rightarrow (\alpha-1)\, x_{MIN}^{\alpha-1} x_{MIN}^{-\alpha} \tfrac{x^{-\alpha}}{x_{MIN}^{-\alpha}} = \tfrac{(\alpha-1)}{x_{MIN}} \left(\tfrac{x}{x_{MIN}}\right)^{-\alpha} \\
&\Rightarrow L(\{\alpha, x_{MIN}\}, x_i) = \textstyle\prod_{i=1}^{N} \tfrac{(\alpha-1)}{x_{MIN}} \left(\tfrac{x_i}{x_{MIN}}\right)^{-\alpha} \\
&\Rightarrow l(.) = \textstyle\sum_{i=1}^{N} \left[\ln(\alpha-1) - \ln(x_{MIN}) - \alpha \ln(\tfrac{x_i}{x_{MIN}})\right] \\
&\Rightarrow l(.) = N\ln(\alpha-1) - N\ln(x_{MIN}) - \alpha \textstyle\sum_{i=1}^{N} \ln\left(\tfrac{x_i}{x_{MIN}}\right) \\
&\Rightarrow \tfrac{\partial l(.)}{\partial \alpha} = \tfrac{N}{(\alpha-1)} - \textstyle\sum_{i=1}^{N} \ln\left(\tfrac{x_i}{x_{MIN}}\right) = 0 \Rightarrow \tfrac{(\alpha-1)}{N} = \tfrac{1}{\sum_{i=1}^{N} \ln\left(\frac{x_i}{x_{MIN}}\right)} \Rightarrow \widehat{\alpha} = \tfrac{N}{\sum_{i=1}^{N} \ln\left(\frac{x_i}{x_{MIN}}\right)} + 1.
\end{aligned}
$$

Funding Open Access funding provided by University of Vaasa. The author declares that no funds, grants, or other support were received during the preparation of this manuscript.

Declarations

Competing interests The author has no relevant financial or non-financial interests to disclose.

References

Andersen, T. G., Bollerslev, T., Diebold, F. X., & Ebens, H. (2001a). The distribution of realized stock return volatility. *Journal of Financial Economics, 61*, 43–76.

Andersen, T. G., Bollerslev, T., Diebold, F. X., & Labys, P. (2001b). Modeling and forecasting realized volatility. *Econometrica, 71*, 579–625.

Andersen, T. G., Bollerslev, T., Diebold, F. X., & Labys, P. (2001c). The distribution of realized exchange rate volatility. *Journal of the American Statistical Association, 96*, 42–55.

Campbell, J. Y., Serfaty-De Medeiros, K., & Viceira, L. M. (2010). Global currencyhedging. *Journal of Finance, 65*, 87–121.

Chen, J., Clements, M. P., & Urquhart, A. (2024). Modeling price and variance jump clustering using the marked hawkes process. *Journal of Financial Econometrics, 22*(3), 743–772.

Chou, R. Y., Chou, H., & Liu, N. (2010). Range volatility models and their applications in finance. In: *Handbook of quantitative finance and risk management*. Springer.

Cirillo, P., & Taleb, N. N. (2020). Tail risk of contagious diseases. *Nature Physics, 16*(6), 606–613.

Clauset, A., Shalizi, C. R., & Newman, M. E. J. (2009). Power law distributions in empirical data. *SIAM Review, 51*, 661–703.

Della Corte, P., Sarno, L., & Tsiakas, I. (2009). An economic evaluation of empirical exchange rate models. *Review of Financial Studies, 22*, 3491–3530.

Fathi, M., Grobys, K., & Kolari, J. W. (2024). On the Realized Risk of Foreign Exchange Rates: A Fractal Perspective. *Journal of Risk and Financial Management, 17*, 79.

Godfrey, L. (2009). *Bootstrap tests for regression models.* Springer.
Grobys, K. (2021). What do we know about the second moment of financial markets? *International Review of Financial Analysis, 78*, 101891.
Grobys, K. (2023). Correlation versus co-fractality: Evidence from foreign-exchange-rate variances. *International Review of Financial Analysis, 86*, 102531.
Grobys, K. (2024). A universal exponent governing foreign exchange rate risks. *International Review of Financial Analysis, 95*(B), 103422.
Grobys, K., & Junttila, J.-P. (2021). Speculation and lottery-like demand in cryptocurrency markets. *Journal of International Financial Markets Institutions and Money, 71*, 101289.
Hou, K., Xue, C., & Zhang, L. (2020). Replicating Anomalies. *Review of Financial Studies, 33*(5), 2019–2133.
Krämer, W., & Runde, R. (1996). Stochastic properties of German stock returns. *Empirical Economics, 21*, 281–306.
Lux, T. (1995). Herd behaviour, bubbles and crashes. *Economic Journal, 105*(431), 881–896.
Lux, T. (2000). On moment condition failure in German stock returns: An application of recent advances in extreme value statistics. *Empirical Economics, 25*, 641–652.
Lux, T., & Alfarano, S. (2016). Financial power laws: Empirical evidence, models, and mechanisms. *Chaos, Solitons and Fractals, 88*, 3–18.
Mandelbrot, B. (1967). The variation of some other speculative prices. *Journal of Business, 40*(4), 393–413.
Opie, W., & Riddiough, S. J. (2020). Global currency hedging with common risk factors. *Journal of Financial Economics, 136*, 780–805.
Parkinson, M. (1980). The extreme value method for estimating the variance of the rate of return. *Journal of Business, 53*(1), 61–65.
Shu, J. H., & Zhang, J. E. (2006). Testing range estimators of historical volatility. *Journal of Futures Markets, 26*, 297–313.
Taleb, N. N. (2010). *The black swan: The impact of the highly improbable.* Random house trade paperbacks.
Taleb, N. N. (2012). *Antifragile: Things that gain from disorder*. Penguin UK.
Taleb, N. N. (2020). *Statistical consequences of fat tails: Real world preasymptotics, epistemology, and applications*. STEM Academic Press.
Uzun, S., Sensoy, A., & Nguyen, D. K. (2023). Jump forecasting in foreign exchange markets: A high-frequency analysis. *Journal of Forecasting, 42*(3), 578–624.
White, E. P., Enquist, B. J., & Green, J. L. (2008). On estimating the exponent of power-law frequency distributions. *Ecology, 89*(4), 905–912.
Yi, C. D. (2020). Jump probability using volatility periodicity filters in US Dollar/Euro exchange rates. *North American Journal of Economics and Finance, 53*, 101184.
Yi, C. D. (2023). Exchange rate volatility and intraday jump probability with periodicity filters using a local robust variance. *Finance Research Letters, 55*(Part A), 103821.
Yi, C. D. (2025). Volatility and jump with intraday periodicity and truncated power variation in Chinese yuan-US dollar exchange rates. *Asia-Pacific Journal of Accounting & Economics, 32*(3), 418–436. https://doi.org/10.1080/16081625.2024.2326408